Performance of Activated carbon Derived from Hydrochar Generated from Processing Wastewater Sludge and Other Waste Biomass in Removing Micropollutants of Concern from Wastewater Effluent.

Prepared by:

Linamandla Ponco

PNCLIN003

Supervised by: A/Prof David S Ikumi

Dissertation submitted in fulfillment of the requirements

For the degree of "Master of Science in Engineering- Water Quality Engineering"

Department of Civil Engineering

University of Cape Town, Private Bag Rondebosch, 7700

South Africa 7700

Abstract

The mass manufacture of novel chemicals, extensive use, and the release of micropollutants into the environment are inevitable occurrences in contemporary society. In reality, wastewater treatment plants are the primary means of spreading micropollutants, primarily because of their inadequate performance. However, efforts are being made to improve their efficiency and achieve an 80% reduction in micropollutant levels. Among the several methods used for the tertiary treatment of wastewater, adsorption stands out for its effectiveness in removing micropollutants. One popular adsorption material is activated carbon, however, the most common commercial version is expensive and made from coal, which is a scarce resource. As a result, we must immediately begin investigating potential substitute precursors that can produce effective activated carbon and are both easily accessible and inexpensive. Because of its high organic content, sludge from wastewater treatment plants is showing promise as an alternative. Stricter disposal restrictions make it more difficult to manage this sludge, a by-product of water treatment. Subsequently, the two varieties of carbon were employed in batch adsorption tests to determine the ideal conditions necessary for each carbon to attain the maximum removal of lead (II) ions from aqueous solutions. This entailed manipulating factors such as pH, adsorbent dosage, initial concentration of the adsorbate solution, and contact time. The optimum conditions that were obtained were 180 min contact time, 300 mg adsorbent dose, and pH of 8. Comparing the results obtained from these tests under optimal conditions for each adsorbent, it was determined that the percentage removal of lead (II) ions was as follows: GAC (99.91%) > HC-PS-WAS-Scr (97.25%), indicating that GAC exhibited a marginally superior performance in the removal of the pollutants compared to the other adsorbents. Adsorption behaviour could be described using the Langmuir and Freundlich isotherm model. Regardless of the adsorbent studied, Langmuir isotherm model fitted well with the adsorption data. The maximum adsorption capacity was found to be 66 mg/g for HC-PS-WAS and 60 mg/g for GAC. The adsorption kinetics could most likely be described with pseudo second order kinetic model for both adsorbents considered.

Acknowledgments

I want to express my deepest gratitude to my supervisor, Assoc. Prof. D.S Ikumi, for welcoming me to his research group and providing me with immense knowledge, expertise and training. The door to his office was always open whenever I needed guidance with regards to my research project t. I really appreciate his constant encouragement, constructive comments and for sharing his pearls of wisdom and assistance during the course of this research. I would also like to thank Dr E. Musvoto and Prof L. Petrik for their invaluable expertise, training and input towards my project, particularly with respect to adsorption studies.

I take this opportunity to express my gratitude to the members of the Water Quality research group for their great ideas and input in our group meetings that encouraged me to think outside the box with respect to my research project. Also, the University of Cape Town for giving me the opportunity to pursue my Master's degree and the Civil Engineering Department for their support, and the facilities they made available for me to be able to get to this final stage of my research.

A special thanks goes to Water Research commission (WRC) for their financial support towards my studies, I would not have been able to pursue this degree if it was not for their continuous support.

Finally, I would like to express my profound appreciation to my mother, siblings and friends for their unfailing support, encouragement and motivation throughout my studies.

Thank you all for your support!

Declaration

I, Linamandla Ponco, possess a comprehensive understanding of plagiarism and hereby affirm that all the content inside this paper, with the exception of correctly recognized sources, is solely my own creation. This thesis/dissertation has undergone scrutiny by the Turnitin module (or a similar software for assessing similarity and originality). I affirm that my supervisor has reviewed my report and any issues identified through this process have been addressed in consultation with my supervisor**.**

Signed by candidate

Signed: **Date : _____12 February 2024____**

Table Of Content

List of Figures

List of Tables

ABBREVIATIONS

AC Activated Carbon

ASTM American Society for Testing and Materials

BET Brunauer-Emmet-Teller

EDS Energy Dispersive X-Ray Spectroscopy

EHTP Enhanced Hydrothermal Polymerization

FT-IR Fourier Transform Infrared

ICP-OES Inductively Coupled Plasma-Optical Emission Spectroscopy

TGA Thermogravimetric Analysis

GAC Granular Activated Carbon

HC-AC-PS-WAS-Scr Hydrochar Derived Activated Carbon, generated from primary sludge (PS), waste activated sludge (WAS), solid screenings of a wastewater treatment plant.

HCL Hydrochloric Acid

HNO3 Nitric Acid

NaOH Sodium Hydroxide

PAC Powdered Activated Carbon

PB Lead

WHO World Health Organization

UV-VIS Ultraviolet- Visible Spectroscopy

WWTP Wastewater Treatment plant

NOMENCLATURE

***C*0** initial concentration in aqueous solution (mol L−1)

***C*t** concentration in solution at any time *t* (mol L−1) **Ce**

equilibrium concentration of the adsorbate (mg/L)

Kf Freundlich constant

***k*1** adsorption rate constant for first-order kinetic equation (min−1) ***k*2**

adsorption rate constant second-order kinetic equation (g/mg min) ***M***

mass of adsorbent (g)

qe equilibrium concentration of metals ions on adsorbent (mg/g)

***q*t** the amount of metals ions adsorbed at any time, *t*(mg/g)

qm Langmuir monolayer capacity of the adsorbent (mg/g)

***R*2** linear regression coefficient

t time (s)

V volume of solution

1 INTRODUCTION

1.1 Background and Motivation

Ensuring adequate access to safe drinking water is a global development issue. However, many countries and large cities around the world continue to experience increasing water scarcity in the twenty-first century. This is largely due to population increase, excessive water use, rising pollution, and changes in weather patterns related to global warming (Grover, 2006). It is exacerbated by a spatial pattern of economic activity and habitation that is fundamentally out of sync with natural water supplies.

Wastewater reuse has been recognized as an encouraging solution to cope with the problem of water scarcity around the globe (Garcia and Pargament, 2015). Some of the strategies that have been implemented to try and alleviate the water scarcity challenge are the recycling and the reuse of effluents generated from wastewater treatment plants. These tactics are becoming an increasingly important aspect of water demand management since it promotes the maintenance of high-quality freshwater sources while also potentially lowering pollution levels and total costs (Jefferson *et al.*, 2000). As part of wastewater treatment processes, micropollutants of concern require removal to ensure that the water quality is of acceptable standard for its re-use. This is achieved *via* the use of wastewater treatment technologies such as membrane bioreactors (Pramodbabu *et al.*, 2021), ultraviolet disinfection (Zaki and El-Gendy, 2014), ozonation and advanced oxidation (Lim *et al.*, 2022). These technologies have been incorporated in current designs of wastewater reclamation and reuse (WR&R) globally. However, they are known to be very expensive and energy-intensive, which places them out of reach for most low and middle-income countries (LMICs) water utilities. Therefore, emerging cost-effective and less energy-intensive treatment technologies have been explored as alternative solutions that can enable the implementation of a sustainable WR&R system.

Tertiary treatment is an additional stage in wastewater treatment processes, whereby the biologically treated effluent goes through further treatment processes. This phase removes nutrients, pathogenic organisms, nonbiodegradable chemicals, heavy metals, leftover inorganic dissolved solids, suspended solids to ensure that the effluent meets the purity requirements for its intended use/re-use. There are various types of tertiary treatment processes such as biosorption, adsorption, oxidation, advanced oxidation, ion exchange as well as membrane filtration and extraction (Gutiérrez *et al.*, 2021).

1.2 Problem statement

Micropollutants classification in wastewater effluents has not changed. These micropollutants frequently encountered include heavy metals (mercury, lead, cadmium, chromium, copper, etc.), organic substances (dyes, solvents, hydrocarbon, etc.) and chemical products (pharmaceutical products, personal care products, etc.) (Rogowska *et al.*, 2020). Moreover, they pose a significant risk to the

environment and human health due to their persistence and potential toxicity (Mariana *et al*., 2021). Conventional wastewater treatment processes consist mainly of preliminary treatment (screening and degritting), primary treatment (primary sedimentation), secondary treatment (biological or chemical treatment, secondary sedimentation), and tertiary treatment (disinfection). They are effective in removing conventional pollutants, such as organic matter, suspended solids, and nutrients. However, they are less efficient in the removal of micropollutants due to their low concentration and complex chemical structures. This limitation necessitates the exploration of advanced treatment technologies to address the issue of micropollutant contamination.

Activated carbon, a highly porous and adsorptive material, has been widely employed in wastewater treatment for the removal of various micropollutants mentioned above (Bhatnagar *et al.*, 2013). There are several types of activated carbon adsorbents, each with specific properties and applications, Granular Activated Carbon (GAC), Coarse particles with sizes ranging from 0.2 to 5 mm. Uses Commonly used in water and air treatment systems. Working Mechanism, GAC adsorbs contaminants from liquids and gases by trapping them in its porous structure. It is effective in removing organic compounds, chlorine, and other pollutants. Powdered Activated Carbon (PAC), Fine powder with particle sizes less than 0.18 mm. Typically used in batch processes for water treatment, including the removal of taste, odor, and organic contaminants. Working Mechanism, PAC is added directly to the medium to be treated, where it adsorbs contaminants. It is then removed by filtration or sedimentation. Biological Activated Carbon (BAC), Similar to GAC but combined with biological treatment processes, Often used in drinking water treatment and wastewater treatment. Working Mechanism: BAC combines the adsorption capabilities of GAC with biological degradation. Microorganisms colonize the carbon surface and degrade adsorbed organic compounds, enhancing the removal efficiency and extending the life of the carbon. Each type of activated carbon is chosen based on the specific requirements of the treatment process, such as the nature of the contaminants, the treatment environment, and the desired outcome. .Its adsorption capacity stems from its extensive internal surface area and diverse surface chemistry, making it suitable for capturing a broad spectrum of pollutants. Traditional activated carbon is typically produced from non-renewable resources, such as coal or wood, which raises environmental and economic concerns. However, hydrochar (biochar), a carbon-rich material produced through the hydrothermal carbonization (HTC) of wet biomass (Yadav *et al.*, 2021) and wastewater sludge, presents a sustainable alternative for activated carbon production. Therefore, hydrochar may be recognized for its potential to serve as a precursor for activated carbon with environmental benefits, such as waste valorisation and reduced greenhouse gas emissions (Ighalo *et al.*, 2022). However, the efficacy of activated carbon derived specifically from hydrochar generated from processing wastewater sludge and other waste biomass in removing these micropollutants remains unclear.

1.3 Research Questions and Hypotheses

The research works toward contributing to the understanding of the potential of activated carbon derived from hydrochar obtained from wastewater sludge and waste biomass in wastewater treatment processes.

Based on the above problem statement, the specific research questions to be addressed include:

(i) What are the optimal activation conditions for producing hydrochar-based activated carbon with enhanced adsorption properties?

(ii) Which adsorption kinetics and isotherms models well describe the removal efficiency of the target micropollutants using the hydrochar-based activated carbon?

(iii) Which methods are most useful towards potential regeneration or reactivation for the spent activated carbon?

This statement could be formulated to a research question and stated that GAC is used as a test material to compare hydro char-based AC

From the investigative research process, valuable insights shall be gained for the development of sustainable and efficient approaches to remove micropollutants of concern, thereby safeguarding water resources and protecting human and environmental health.

1.4 Research aim and objectives

The overarching aim of this study is to investigate the performance of activated carbon, derived from hydrochar, in removing heavy metals of concern from the effluents of wastewater treatment systems. Hence, the study will involve the characterization of the activated carbon and the evaluation of its adsorption capacity for highly hazardous heavy metals commonly found in wastewater. The following are the specific research objectives:

- Determination of the physico-chemical characteristics of activated carbons from wastewater sludge based hydrochar.
- Determination of optimal activation conditions for batch pyrolysis of both types of hydrochar, generated from primary sludge (PS), waste activated sludge (WAS), solid screenings of a wastewater treatment plant.
- Determining the adsorptive potential for the sludge-generated hydrochar for different types of micropollutants (mainly heavy metals).
- Comparison of adsorptive properties of activated carbons produced by sludge generated hydrochar, with a commercial-grade carbon.

1.5 Scope and Limitations of the Thesis

The objective of this research is to examine wastewater to assess the effectiveness of wastewater sludge-based activated carbon as an adsorbent in removing lead. The wastewater used in the study was artificially synthesized in the laboratory. Batch experiments were carried out with synthetic solutions containing lead ions. The study explored the impact of pH, contact time, initial metal ion concentration, temperature, and adsorbent concentration to optimize the conditions for the maximum removal of lead ions. The experimental data obtained were analyzed and fitted using adsorption isotherms, and various kinetic models. Additionally, water quality analysis of the heavy metals was performed using Inductively Coupled Plasma (ICP).

1.6 Thesis outline

This thesis is organized into five chapters to systematically address the research objectives and provide an extensive understanding of the topic Figure 1.1 portrays the outline of this work. Chapter 2 presents a thorough review of the literature related to micropollutants in wastewater, conventional wastewater treatment methods, The use of activated carbon in wastewater treatment, hydrochar as a precursor for activated carbon, and previous studies on hydrochar-derived activated carbon for heavy metal removal specifically. Chapters 3 and 4 describe the materials and methods, experimental procedures, results, discussions. Finally, Chapter 5 summarizes the key findings, contributions, and future research directions.

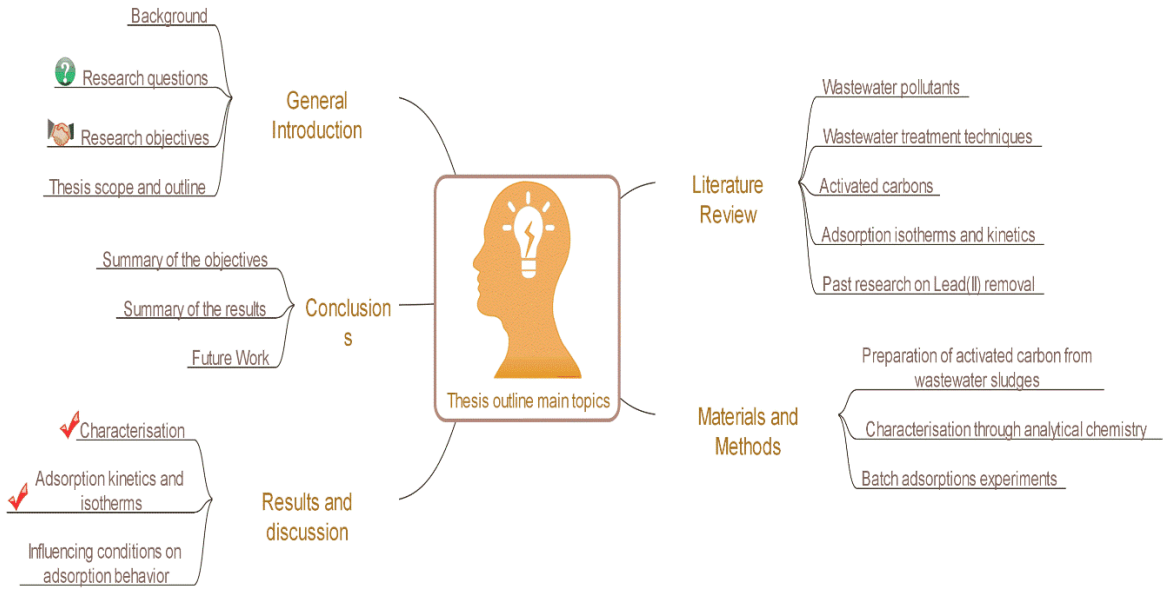

Figure 1-1:Mind map of the thesis outline and different broached topics in this research.

Through this research, we aim to contribute to the growing body of knowledge on sustainable wastewater treatment and the removal of heavy metal, ultimately advancing environmental protection and public health efforts.

2 LITERATURE REVIEW

Water is used in industrial processes. These processes generate useful products and toxic wastes as a byproduct. Industrial waste is often sent to WWTP for further treatment before discharge into the environment. However, the challenge is that industrial wastes are generally difficult to treat in comparison to domestic wastewater . **Figure 2.1** Exhibits the impact of industrial products entering the aquatic environment on aquatic life

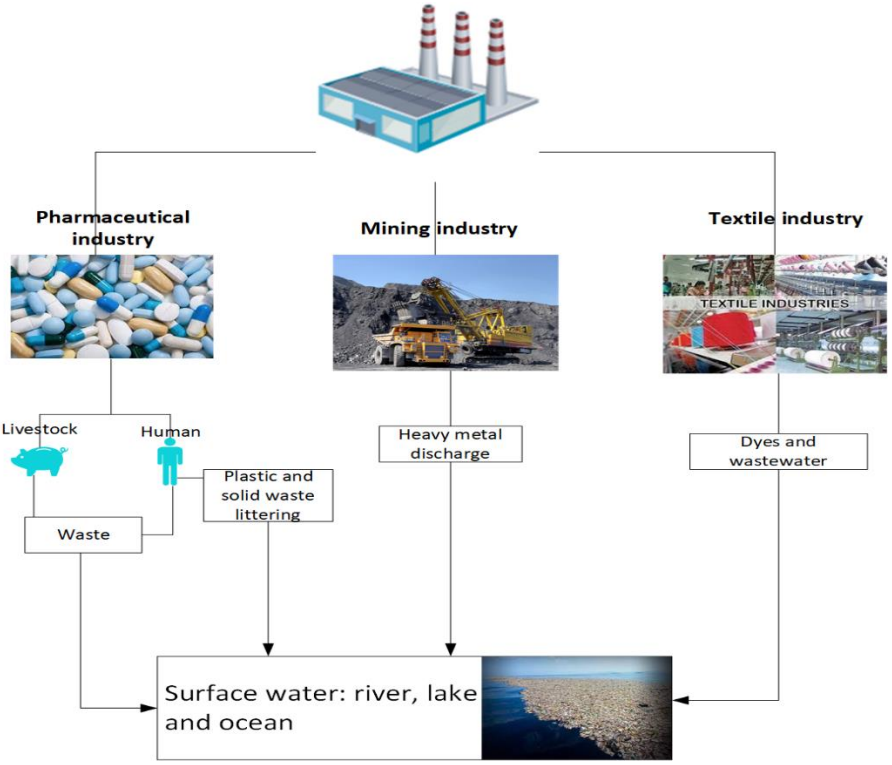

Figure 2-1:Life cycle of water utilization in several industrial sectors

Numerous pollutants, such as hazardous chemicals, pathogenic bacteria, putrescible organic waste, fertilizers, and plant nutrients, can pollute water bodies; hence interfere with the water's ability to be used for good or with ecosystems' ability to function naturally (Gravel, 2020).

2.1 Water pollutants

The inventory of different pollutants produced nowadays is difficult to establish. However, more than 70,000 different chemical products are produced today in the chemical industry, with an estimated $500 billion in global sales are regarded as emerging pollutants in the aquatic environment and have drawn growing attention (Rogowska *et al.*, 2020). Water pollutants can be classified in four groups, namely

pharmaceutical products, dyes, heavy metals and solid wastes such as plastics. Figure 2.2 depicts such a classification(Tchobanoglous, 1991).

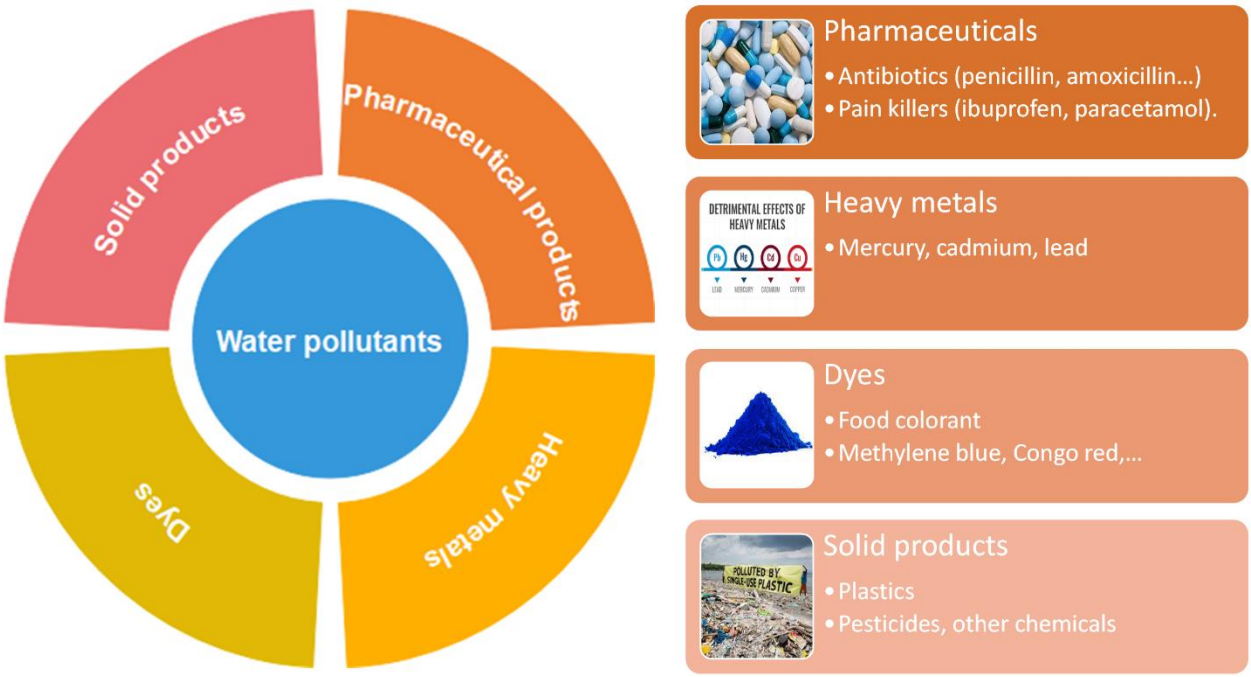

Figure 2-2:Classification of water pollutants

Due to their strong polarity and low volatility, most pharmaceutical products tend to be easily carried and discharged into the water compartment (Breton and Boxall, 2003). To the great worry of scientists, numerous chemicals present in wastewater effluents and/or their metabolites and transformation products are detected in surface waters and end up in marine environments (HELCOM, 2003, Pastuszak *et al.*, 2018). Although pharmaceutical substances are necessary in contemporary life (e.g., the widespread use of antibiotics, and hormones in the swine industry), their discharge into the aquatic environment can have several negative consequences and thereby ruin the ecology(Cheng *et al.*, 2020).

Numerous industrial sectors, including the agroindustry, petroleum, and leather industries, are likely to produce highly saline wastewater. It is known that releasing wastewater with such a high salinity and high organic content without first treating it has a negative impact on aquatic life, water potability, and agriculture. As a result, laws are getting stricter, and many nations now require the treatment of saline wastewater for both the removal of organic matter and salt. Saline effluents are often treated using physico-chemical methods since salts severely hinder biological treatment (mainly NaCl) (Lefebvre and Moletta, 2006). Alternative systems for the treatment of organic matter are currently the subject of research to a greater extent due to the high costs of physio-chemical treatment processes. Even though it has been demonstrated that biological treatment of carbonaceous, nitrogenous, and phosphorous pollution is possible at high salt concentrations, the effectiveness attained depends on the biomass's suitability for halophilic organisms or other modifications (Lefebvre and Moletta, 2006).

Heavy metals are another class of important water contaminants . The main reason of the rising levels of heavy metals observed in aquatic ecosystems is identified as anthropogenic activities. These activities include tanneries, metal mining, plating, painting, and radiator manufacture, which are major drivers of water pollution because their effluents include heavy metals. Heavy metals in high quantities in water supplies can generate a variety of difficulties for the environment and living things. According to the World Health Organization (WHO), there exists a permissible concentration of heavy metals in water usage(Qasem *et al.*, 2021). **Table 2.1** lists the main sources of heavy metals and their deleterious effects on human bodies. As a result, the removal of heavy metals from wastewater has been the topic of tremendous research efforts (Sellaoui *et al.*, 2017).

Table 2-1: Most dangerous heavy metals encountered in wastewater (Qasem et al., 2021, Mariana et al., 2021)

Common heavy metal	Main sources	Health issues	Permitted amount (μg/L)
Cadmium (Cd)	-batteries; paints; metal refineries	Acute toxicity with headaches, skin ulcers, dermatitis nausea, diarrhea, and cancers.	3
Lead (Pb)	Lead-based batteries; solder, alloys, cable sheathing pigments, rust inhibitors, ammunition, glazes, and plastic stabilizers.	Neuro degenerative diseases, Alzheimer's disease, and senile dementia, kidney damage, and cancers	50
Mercury (Hg)	Production of chlorine; Caustic soda; refineries	Effects on digestive system, impaired neurologic development and hypertension.	1
Arsenic (As)	Electronics and glass production.	Skin, lungs, brain, kidneys, metabolic system, cardiovascular system, immunological system, and endocrine.	50

Nickel (Ni)	Stainless steel and nickel alloy production	Lung, kidney, gastrointestinal distress, pulmonary fibrosis, and skin.	70
Chromium (Cr)	Steel and pulp mills and tanneries.	Skin, lungs, kidneys, liver, brain, pancreas, tastes, gastrointestinal system, and reproductive system	50

Dyes are one of the oldest and most widely used substances in a variety of industries, including textiles, plastics, and printing. Giving the different colors dyes have, their detection in wastewater can be perceivable even in a slightest concentration. As a result, their presence in water can obstruct (diffraction) light diffusion or oxygen provision to underwater organisms thereby disrupting aquatic life. Furthermore, dyes are regarded the most dangerous water contaminants given their carcinogenicity, non-biodegradability, and high toxicity even in small amounts. The high toxicity of dyes comes from their aromatic structure (benzoic ring)(Hunger, 2003) as shown in **Figure 2.3**.

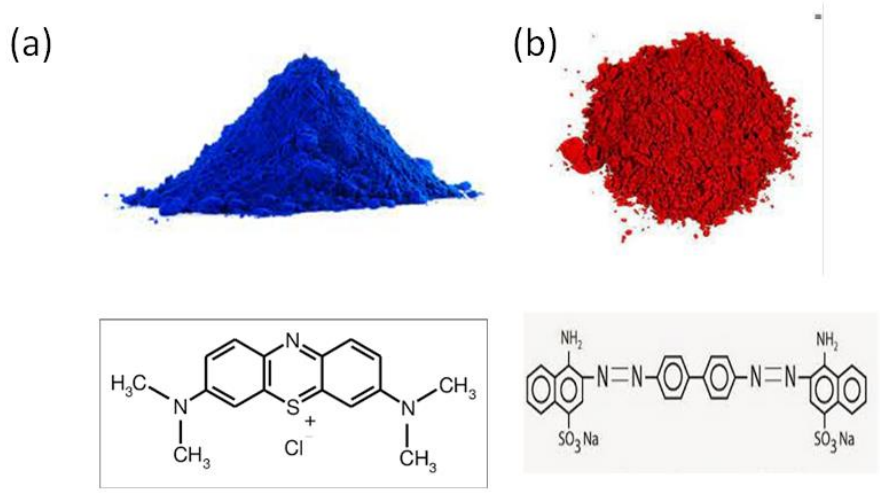

Figure 2-3:Selected industrial dyes: (a) Methylene Blue, (b) Congo Red

2.2 Techniques of wastewater treatment

Wastewater usually contains a combination of organic, inorganic, soluble and insoluble compounds. Therefore, the selection of a method of treatment should be based on the efficacy of pollutant removal and most importantly on economic feasibility. Several researchers have committed their efforts to developing unique tertiary wastewater treatment procedures due to the environmental concerns sparked by water pollution (Moussa *et al.*, 2017). Adsorption, membrane filtration, coagulation/flocculation,

oxidation, and biological treatment are some technologies that have been developed to reduce wastewater discharges and decrease the risks of pollutants (Xu, 2018). **Figure 2.4** depicts some of these treatment methods.

2.2.1 Physical methods of wastewater treatment

These are methods that allow for wastewater treatment without a chemical modification of all the organisms present within.

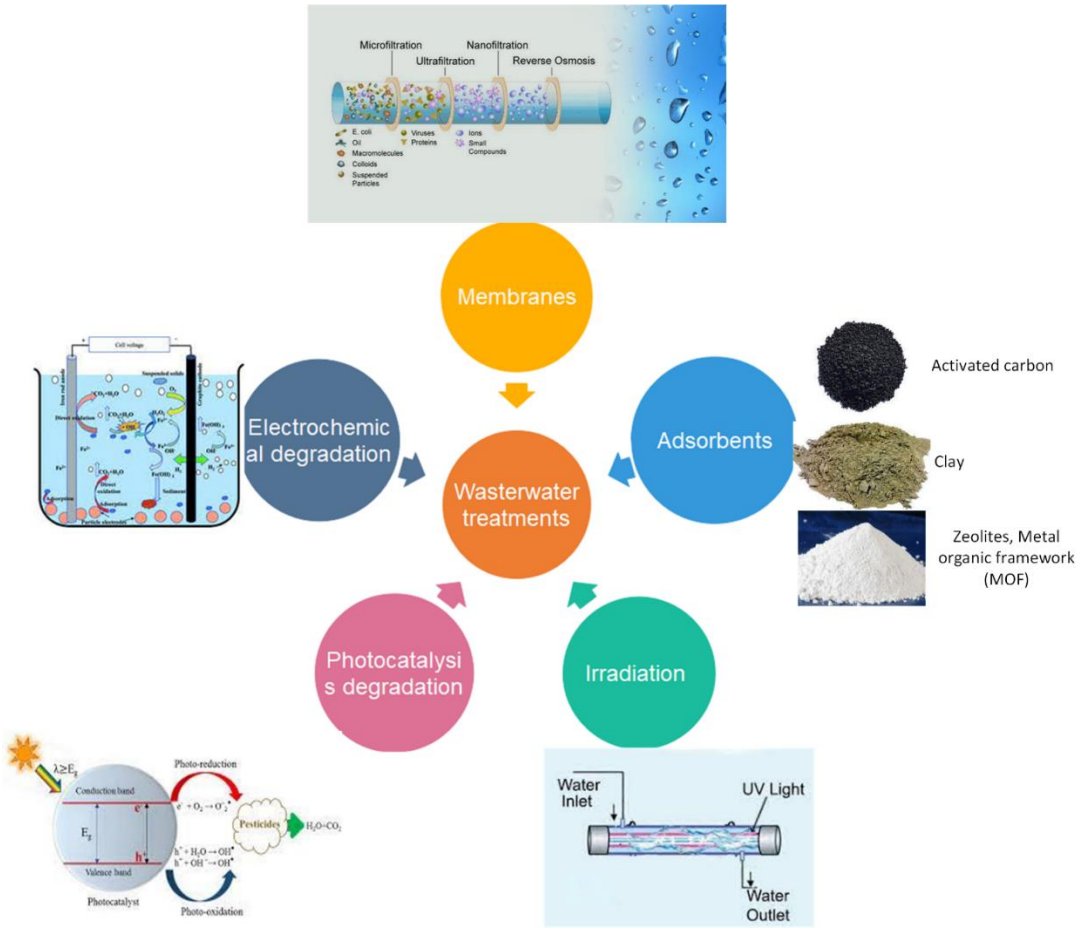

Figure 2-4: Wastewater treatment techniques

2.2.1.1 Adsorbents

Adsorption is a mass transfer process whereby a solute or removably-occurring species is moved from a liquid phase to the surface of a solid phase. Adsorbed organisms are attached to the solid surface through physiochemical interactions (Manchisi *et al.*, 2020). Adsorbate migration in this process typically takes place in three processes that happen in succession, migration of the adsorbate to the adsorbent's border shell, intraparticle diffusion into pores, and solute adsorption and desorption (Yue *et al.*, 2020). Due to its simplicity and affordability in comparison to the other methods, adsorption is

regarded as a well-developed procedure for removing colors from wastewater(Slatni *et al.*, 2020). Various researchers have recently focused on finding adsorbents with huge surface areas, low costs, and environmental friendliness. For example, the effective adsorbents in nanoscale materials, which have been crucial for removing colors, heavy metals, organic chemicals, etc. from wastewater (Moussa *et al.*, 2017).

2.2.1.2 Membranes

Membrane filtration is one of the most influential and cost-effective methods for separating or removing colors and organic materials in wastewater. The creation of membranes with enough thermal stability and enhanced performance is still a difficult task. The membranes' rejection, permeability and antifouling performance can be influenced by its hydrophilicity and surface charge (Yang *et al.*, 2020).

Nanofiltration: The use of nanofiltration (NF) technology as a purification and separation technique for wastewater treatment has been demonstrated to be effective. Concentration polymerization and fouling, however, may significantly limit the NF membrane's performance. The membrane's permeability is reduced by fouling because it blocks membrane pores by accumulating an organic coating. Also, because salt rejection raises the osmotic pressure, high salinity deleteriously impacts on membrane flow. Therefore, a membrane with the hydrophilic surface is preferred for the treatment of textile wastewater under high throughputs (Liang *et al.*, 2020).

Ultrafiltration: Due to its ability to provide high salt penetration with increased permeation flux, the ultrafiltration (UF) technology is gaining popularity in the dyeing and salt fractionation industries. Studies comparing different membranes show that UF membranes have a high separation efficiency due to more excellent salt permeability and the ability to maintain high throughputs under low osmotic pressure. Numerous polymeric materials incorporating polyacrylonitrile (PAN), polysulfone (PSf), cellulose acetate (CA), polyethersulfone (PES), and poly(vinylidene fluoride) (PVDF) have been employed and thoroughly investigated in order to create effective UF membranes (Baresel *et al.*, 2019).

2.2.1.3 Coagulation/flocculation

For the decolorization of wastewater containing dispersion dyes, coagulation-flocculation techniques are adequate. Dye solution systems are destabilized during coagulation to generate flocs and agglomerates. The flocculation process involves stabilizing the suspended particles and combining flocs into more oversized agglomerates that sink under the pull of gravity (Lee *et al.*, 2012, Zahrim *et al.*, 2011). By linking or trapping the suspended particles arranged into gelatinous agglomerates that are large enough to be limited in the filter or settle down, the coagulation-flocculation process is used to counterbalance charges. Since coagulation-flocculation is an economically viable method with a quick detection time and straightforward operation, it is frequently used in the textile industry to treat wastewater. In these techniques, coagulants like lime ($Ca(OH)_2$), ferric chloride ($FeCl_3 \cdot 7H_2O$), ferric sulfate ($Fe_2(SO_4)_3 \cdot 7H_2O$), and aluminum sulphate ($Al_2(SO_4)_3 \cdot 18H_2O$) bind with the pollutants and other

dispersed dyes to remove them, through the action of sorption, electrostatic force and bridging. Due to the protonated amine groups and polymer (high molecular weight), sorption and bridging, aid in the coagulation of flocculating colors and contaminants from wastewater. The wastewater discharge is reduced by coagulation and flocculation of dissolved chemicals, suspended matter, colloidal particles, non-settable particles, and coloring agents (Yogalakshmi *et al.*, 2020).

2.2.2 Chemical methods of wastewater treatment

Generally, in these cases, the chemical structure of contaminants is altered by the aid of a catalyst or the addition of electrons from electricity or light.

2.2.2.1 Electrochemical degradation

Electrochemical degradation is a process by which wastewater is directly or indirectly oxidized by the supply of a direct current (DC) power. The provision of electrons in the wastewater solution oxidizes/reduces the species present to intermediates species. The efficiency of the treatment can be improved by the selection of appropriate electrodes and the voltage. Fan *et al.*(Fan *et al.*, 2008) investigated the electrochemical degradation of aqueous solution of Amaranth azo dye on activated carbon fiber (ACF) electrodes under potentiostat model. They found that the adsorption on the electrodes was insignificant. However, the success of removal of the color and the chemical oxygen demand (COD) were demonstrated when a properly selected voltage region was chosen. What is more, a relationship between the discoloration and the applied voltage was established. Ceron-Rivera *et al.* (Cerón-Rivera *et al.*, 2004) studied the degradation of textile dyes (Basic yellow 28 and Reactive black 5) using diamond, aluminum, copper, iron and zinc electrodes. The electrochemical degradation was conducted in different potential ranging from -1 to -2.5 V. The results showed that 95 % of wastewater color was removed and the COD removal was up to 67%. In other cases, the addition of other energy sources such as ultrasound can be conducted to enhance the dye removal (Yang *et al.*, 2014). Naumczy *et al.* (Naumczyk *et al.*, 1996) performed an electrochemical treatment of textile wastewater in the presence of high concentration of chlorine ions using Titanium/ruthenium oxide (Ti/RuO_2), Titanium/Platinum (Ti/Pt) and Titanium/Platinum/ Iridium (Ti/Pt/Ir) electrodes. All the anodes proved their effectiveness in the direct and indirect oxidation of organics inside the wastewater. After an hour of electrolysis at $6A/dm^2$ the COD was reduced by 85-92 %.

2.2.2.2 Photocatalytic degradation and irradiation

Photocatalytic degradation is a process whereby a photocatalyst is used to break down and remove organic pollutants and other harmful substances present in wastewater. This process involves the use of an electromagnetic light source to activate the photocatalyst, which then reacts with the pollutants in the water, breaking them down into harmless components (Soltani *et al.*, 2012).

The photocatalytic degradation process typically involves the use of a semiconductor material, such as titanium dioxide or zinc oxide, as the photocatalyst. When light is absorbed by the photocatalyst, it creates electron-hole pairs, which then split water molecules in highly reactive hydroxyl radicals. These hydroxyl radicals then react with the organic pollutants in the wastewater, breaking them down into smaller, less harmful compounds. Using oxides as semiconductor have the advantage of high stability in water. However, because of their wide band gap, TiO_2 (3.3 eV), ZnO (3.4 eV) or Fe_2O_3 (2.67 eV), they can only be activated with ultraviolet light, which may decrease their overall degradation efficiency (Chakraborty *et al.*, 2022). To alleviate this limitation, several researchers have used semiconductors, such as copper selenide (CuSe, Cu_2Se, $CuSe_3$) that can be activated by visible light (Farooq *et al.*, 2023).

Photocatalytic degradation is a promising technology for the treatment of wastewater because it is an environmentally friendly and cost-effective process. It has the potential to remove a wide range of pollutants, including organic contaminants, bacteria, and viruses, from wastewater without producing harmful byproducts or requiring the use of chemicals (Soltani *et al.*, 2012).

Irradiation of wastewater refers to the use of ionizing radiation, such as gamma rays (Ling *et al.*, 2022, Hina *et al.*, 2021) or electron beams, to treat and disinfect wastewater. This process involves exposing the wastewater to a source of ionizing radiation, which can kill microorganisms and break down harmful pollutants present in the water (Son and Lee, 2016). The ionizing radiation causes the formation of highly reactive species, such as hydroxyl radicals, which react with and break down the organic compounds present in the wastewater. The radiation also damages the genetic material of pathogenic microorganisms present in the water, killing them and preventing them from reproducing.

Irradiation of wastewater is a promising technology for the treatment of wastewater because it is an effective and environmentally friendly process. It can remove a wide range of pollutants and microorganisms, including bacteria, viruses, and parasites, from the wastewater without producing harmful byproducts or requiring the use of chemicals. However, it should be noted that irradiation of wastewater requires careful handling to ensure safety for both operators and the environment (Zaki and El-Gendy, 2014).

2.3 Limitations of these Techniques

Table 2.2 displays some non-exhaustive advantages and disadvantages of different techniques of wastewater treatment. Chemical procedures are straightforward, quick, effective, and have a variety of oxidation methods, based on formation of oxidants. In addition to all these characteristics, chemical procedures are typically presented at laboratory-scale and found to be economically unviable for small industries to meet their energy needs(Gutiérrez *et al.*, 2021). Physical methods like membrane filtration are quick and simple even at high concentrations(Xiao *et al.*, 2019). They are thought to be useful for practically all forms of contaminants, including suspended particles, mineral ions, and dyes. Contrary to chemical methods, physical methods require an extensive amount of energy, maintenance, and

operating costs, making them impractical for small businesses. When concentrations are high, membrane blockage (fouling) happens. Coagulation and flocculation are straightforward physiochemical processes. However, managing sludge volume creation (big size flocs) raises the cost of the operations. The public wells adopt biological treatment since it is an easy and appealing procedure from an economic standpoint. However, it takes a long time, degrades slowly, and necessitates the maintenance of healthy microbes in an ideal habitat. After examining several wastewater treatment methods, it is concluded that adsorption is a non-destructive, technologically straightforward, effective, and economical method. It very effectively removes different pollutants from water and wastewater, such as colors, metal ions, minerals, and other impurities (Crini *et al.*, 2019).

Table 2-2:comparative analysis of different techniques of wastewater treatment

Techniques	Advantages	Disadvantages
Membranes	-Can be produced at an industrial scale	-Membrane fouling - High operating cost -decrease of membrane efficacy
Adsorbents	Low cost	Low removal efficiency
Electrochemical degradation	-High efficiency -Low energy consumption -Used for wide range of pollutants	-High capital cost -Requires a skilled personal
Photocatalytic degradation and irradiation	-Low energy consumption - Wide range of pollutants	-Low removal efficiency -High capital cost for semiconductors

2.4 Activated carbons.

Activated carbon (AC) is by definition a black solid material with amorphous crystal structure or less graphite-like crystalline structure. It is an effective adsorbent for removing a wide range of organic and inorganic pollutants from aqueous or gaseous media. Due to its distinct properties, it is increasingly used in air filtration, wastewater treatment, and water treatment (Kosheleva *et al.*, 2019, Samsuri *et al.*, 2014, Youssef *et al.*, 2019). The main property of AC is its porosity. The porosity is the combination of channels and cavities that can accommodate or let through a fluid (gas or liquid). **Figure 2.5** portrays the SEM (scanning electron microscopy) of an AC.

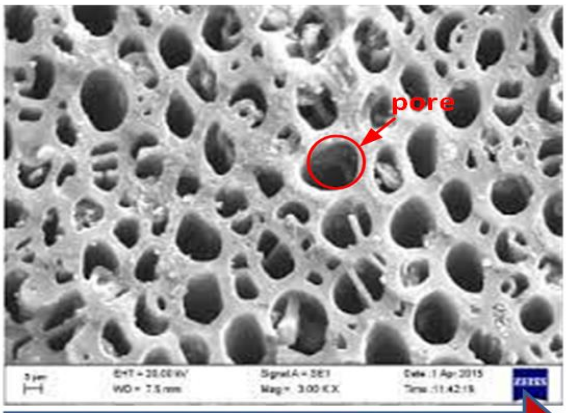

Pore surface area (m^2/g)	600 – 1900	20 – 70	0.5 – 2
Pore volume (cm^3/g)	0.1	0.2	0.2 – 0.8
Pore diameter (nm)	< 2	2 – 50	> 50

Figure 2-5:Scanning electron microscopy (SEM) and pore characteristics of an activated carbon

The SEM allows to see the morphology of the AC. As can be seen, the AC contains many pores with different sizes (volume and surface). The porosity can be classified in three categories depending on the pore dimension: macropores >50 nm, mesopores ranging from 2 to 25 nm, and micropores <2 nm (Huang *et al.*, 2014).

The pore characteristics of the AC strongly depends on its synthesis route. The diagram chart of the AC synthesis is given in **Figure 2.6**. It consists of three main steps, the selection of the precursor, its carbonization, and its activation, with an intermediary step which is the pre-treatment (washing, crushing, and drying the precursors).

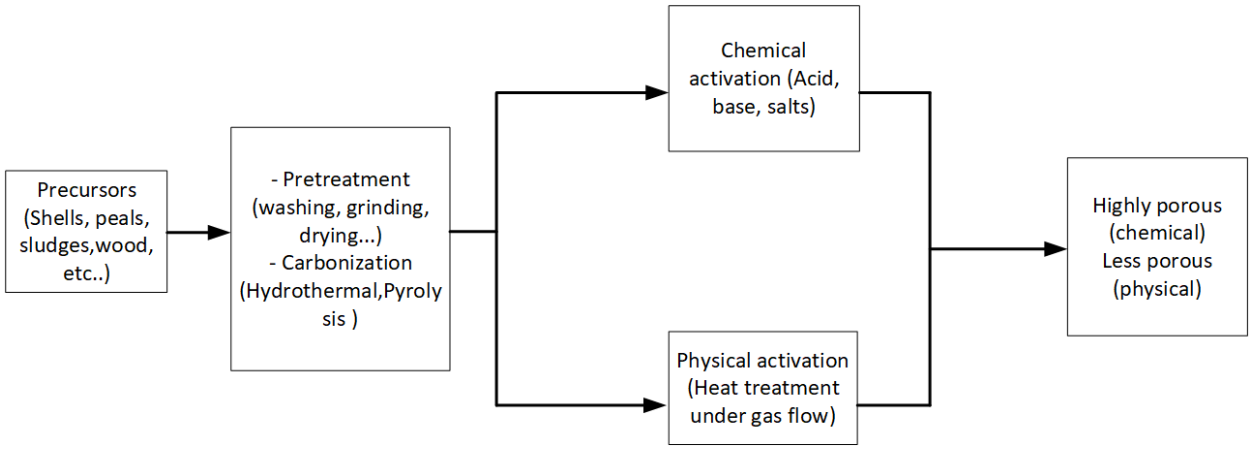

Figure 2-6:Synthesis steps of the activated carbon

The elemental analysis of an AC shows that the carbon content depends generally on the nature of the precursor. This precursor can be further divided in solid (shells, charcoal, wood, etc.) or mushy (sludges). A solid precursor could use to create activated carbon in two steps by (i) carbonizing at high temperatures (pyrolysis; Huang *et al.*, 2014) and (ii) activating it (Byamba-Ochir *et al.*, 2016). During the carbonization process, the material should be subjected to a red spot temperature (less than 700 °C) in distillation apparatus in order to evaporate and remove the hydrocarbons from it in the absence of oxygen. This results in carbonized material, known as char, or biochar (Yahya *et al.*, 2015).

Given the nature of the activation process, there are two ways to prepare activated carbon: physically and chemically.

Physical activation is a two-step process that involves carbonization (pyrolysis) in a neutral atmosphere, followed by activation in atmospheric oxidizing gases such as steam, carbon dioxide, carbon monoxide, and nitrogen, or air mixtures with increasing temperature in the 800-1100 °C range (Bouchelta *et al.*, 2008). This method can produce activated carbon with a porous structure and high physical power at a low cost, and it is considered a green approach because it is chemical-free (Byamba-Ochir *et al.*, 2016, Pallarés *et al.*, 2018, Yahya *et al.*, 2015). However, the main disadvantages of the physical activation of activated carbon are the long activation time, the low adsorption capacity of prepared activated carbon, and high energy consumption (Yahya *et al.*, 2015).

Chemical activation, also known as wet oxidation, is commonly used for cellulose-containing raw materials such as wood, sawdust, or fruit pits. These materials are also known as biomass resources. Organic precursors are activated in the presence of chemicals at high temperatures during chemical activation to produce activated carbon (Njoku *et al.*, 2014, Samsuri *et al.*, 2014, Yahya *et al.*, 2015). In the first stage of chemical activation, the raw material is saturated with oxidizing and highly dehydrated chemicals. Following impregnation, the suspension is dried, and the remaining mixture is heated for a specified period. Depending on the activating material and the final product properties, activation can occur at temperatures ranging from 400 to 900 °C, where cellulose is degraded. Activated carbon is eventually obtained by repeatedly washing the resulting mixture. The recovery of active substances is another goal of the final rinse(Samsuri *et al.*, 2014).

Chemical activation agents are dehydrating agents that affect pyrolytic decomposition and, by preventing the formation of bitumen, increase the activated carbon content, changing the thermal degradation of precursors in the process (Gratuito *et al.*, 2008, Molina-Sabio and Rodríguez-Reinoso, 2004). This causes the porous structure of carbon materials to develop. In addition, the creation of tiny holes in the activated carbon caused by these activating chemicals, which deeply penetrate the carbon structure, increases the surface area of the carbon (Gratuito *et al.*, 2008). Chemical activation differs from physical thermal activation in that the phenomena of carbonization and activation happen simultaneously. As a result, unlike physical activation, which typically performs the carbonization and

activation processes in two different furnaces, chemical activation can be done in just one (Samsuri *et al.*, 2014). The amount of impregnation and the weight ratio of chemical agents to dry precursor are the factors that influence the features of the final activated carbon during the chemical activation process (Gratuito *et al.*, 2008). Due to its lower activation temperature, quicker processing, and higher carbon efficiency compared to physical activation, this activation method is more environmentally friendly (Rambabu *et al.*, 2015).

Surface modifications: The AC surface can be altered by introducing agents that enhance the AC adsorption performance in specific applications. The modification adds to the AC surface some functional groups that interact with the contaminants. Among these agents, oxidizing agents are the most employed in wastewater treatment. Oxidizing agents such as nitric acid, sulfuric acid hydrogen peroxide, introduce oxygen-containing functional groups onto the activated carbon surface, including carboxyl, hydroxyl, and carbonyl groups (Rivera-Utrilla *et al.*, 2011). On the other hand, amines and ammonia impregnation can introduce nitrogen-containing functional groups onto the activated carbon surface, such as amine and amide groups(Bhatnagar *et al.*, 2013, Jansen and van Bekkum, 1994).

2.5 Adsorption process

The adsorption process is generally divided into physisorption and chemisorption. In physisorption, the adsorbate molecules adhere to the adsorbent's surface (AC) with a weak interaction force, usually the electrostatic Van der Waal's forces. The strength of the adhesion depends upon the adsorbent's surface area and chemistry, the temperature, the concentration of the adsorbate and much more. Conversely, chemisorption is characterized by a strong chemical bond existing between the adsorbate molecules and the adsorbent ones. As a result, the strength of adhesion in this case is stronger than that of physisorption. For wastewater treatment applications, the most encountered adsorption process is the physisorption. Therefore, in the following, only the physisorption will be considered. We can further divide the physisorption in two categories depending on the nature of the adsorbate: gas adsorption(Brunauer *et al.*, 1938) and aqueous adsorption (batch adsorption)(Giles *et al.*, 1974).

To understand the adsorption process, one has to identify the different mechanistic steps happening onto the surface of the adsorbents. The adsorption process occurs in 3 steps, generally as depicted in **Figure 2.7**. In the first step (**Figure 2.7a**), the adsorbate molecules fill one by one the pore of the adsorbent surface; this is a monolayer filling. It should be noted in this step there is no interaction between adsorbates and the concentration of these molecules on the adsorbent surface is usually small. Increasing the concentration of adsorbates molecules leads to interaction between pores filling start occurring (**Figure 2.7b**). Further increasing of the adsorbate brings about a condensation process where many layers start piling up on the adsorbent surface (**Figure 2.7c**).

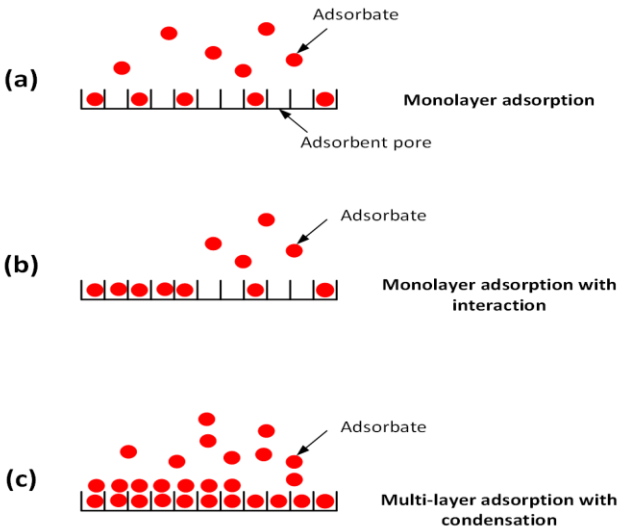

Figure 2-7:Different adsorption mechanistic steps

2.5.1 Mathematical model of adsorption isotherms

2.5.1.1 Adsorption in gas phase

The mathematical model of the adsorption of gas on solid absorbent has been developed in early 1900 by Langmuir (Langmuir, 1918) and has been further elaborated by several researchers among them Brunauer, Emmett, and Teller (BET) (Brunauer *et al.*, 1938) . The BET equation is nowadays widely utilized to characterize nano-particles adsorbents. The equation gives a relationship between the adsorbate (gas) concentration (volume) as a function of relative gas pressure at constant temperature. This equation can be generally expressed as follows:

$$\frac{V}{V_m} = f\left(\frac{P}{P_0}\right) \tag{2.1}$$

Where, V_m is the maximum adsorbed volume of the adsorbate, P is the pressure of adsorbate and P_0 is the reference pressure (P_0 = 1 bar). The mathematical expression of adsorption isotherm can be derived from kinetic modeling or statistical thermodynamic. However, the derivation of these isotherms using this formalism is outside the scope of this work.

Adsorption isotherms for gas phase was classified by (Brunauer *et al.*, 1938). **Figure 2.8** portrays the two main types of isotherms. Adsorption isotherms aid in the selection of adsorbents for specific applications by calculating surface area and adsorption capabilities, as well as the volume and distribution of pores.

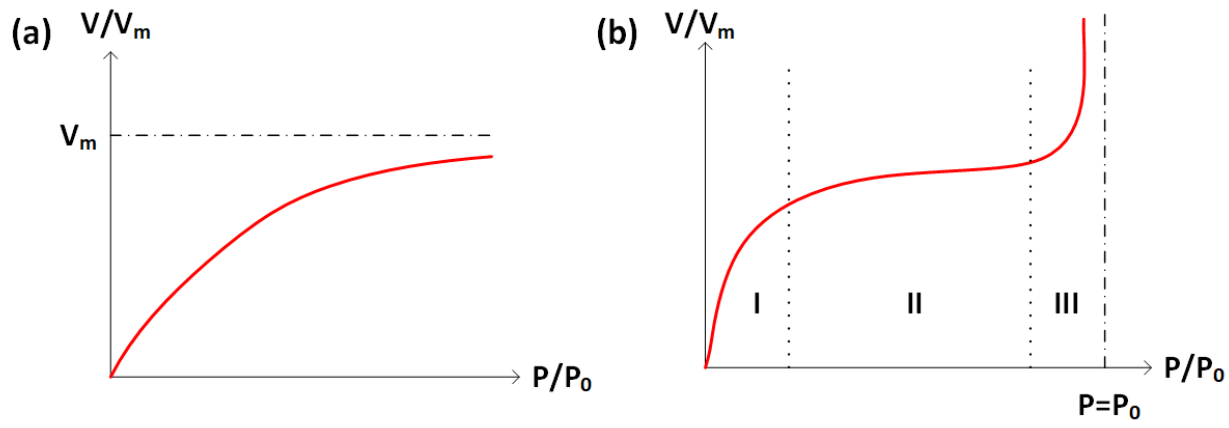

Figure 2-8:gas phase adsorption isotherm: (a) monolayer adsorption (Langmuir model), (b) multilayer adsorption isotherm (BET model), the three zones in the figure correspond to the mechanistic steps of the adsorption process from Figure 2-7.

Originally, Langmuir(Langmuir, 1918) developed his kinetic equation to account for gaseous adsorption, assuming that adsorption was limited to a single molecular level and the adsorbent gas was an ideal gas adsorbed onto an idealized surface. As the first theoretically developed adsorption isotherm, this model laid the foundation for many subsequent theories. The volume of gas uptake on the adsorbent surface is deduced to be:

$$\frac{V}{V_m} = \frac{B\left(\frac{P}{P_0}\right)}{1+B\left(\frac{P}{P_0}\right)} \tag{2.2}$$

Where B is a constant depending on the adsorption energy, the temperature and so on.

On the other side, The BET equation is used to describe multilayer adsorption and was based on Langmuir's model. It is assumed that: (i) Only the first layer of adsorbate molecules is bound to the adsorbent surface by Van der Waal's forces; (ii) Subsequent layers are not bound by Van der Waal's forces and so have the same characteristics as in a liquid state; (iii) For all layers above the first monolayer, the heat of adsorption (of the adsorbate) equals the heat of condensation (of the adsorbate), and (iv) at saturation pressure, an endless (infinite) number of layers can be adsorbed onto the adsorbent surface (**Figure 2.7c**).

As a result, the linearized BET model is as follows:

$$\frac{1}{V\left(\frac{P_0}{P}-1\right)} = \frac{1}{V_m K} + \frac{K-1}{V_m K}\left(\frac{P}{P_0}\right) \tag{2.3}$$

Where *K* is the BET constant related to the enthalpy of adsorption, V_m is the volume of adsorbate (gas) to form a monolayer. The plot of $\frac{1}{V\left(\frac{P_0}{P}-1\right)}$ against P/P_0 is a linear plot with $(K-1)/V_mK$ as a slope and $1/V_mK$ the intercept.

2.5.1.2 Batch adsorption process (Aqueous)

When the adsorption of solute (adsorbate) on solid particles (adsorbent) is investigated, the adsorbate concentration in a known volume of solution C (mg/L or mol/L) is compared to the amount of adsorbate per unit mass of adsorbent *Q* (mg/g). The mathematical relationship between *Q* and *C* at a fixed temperature $Q=f(C)$ is called batch adsorption isotherm. Giles *et al.*(Giles *et al.*, 1974) were the first to classify these types of isotherms which are plotted in **Figure 2.9**.

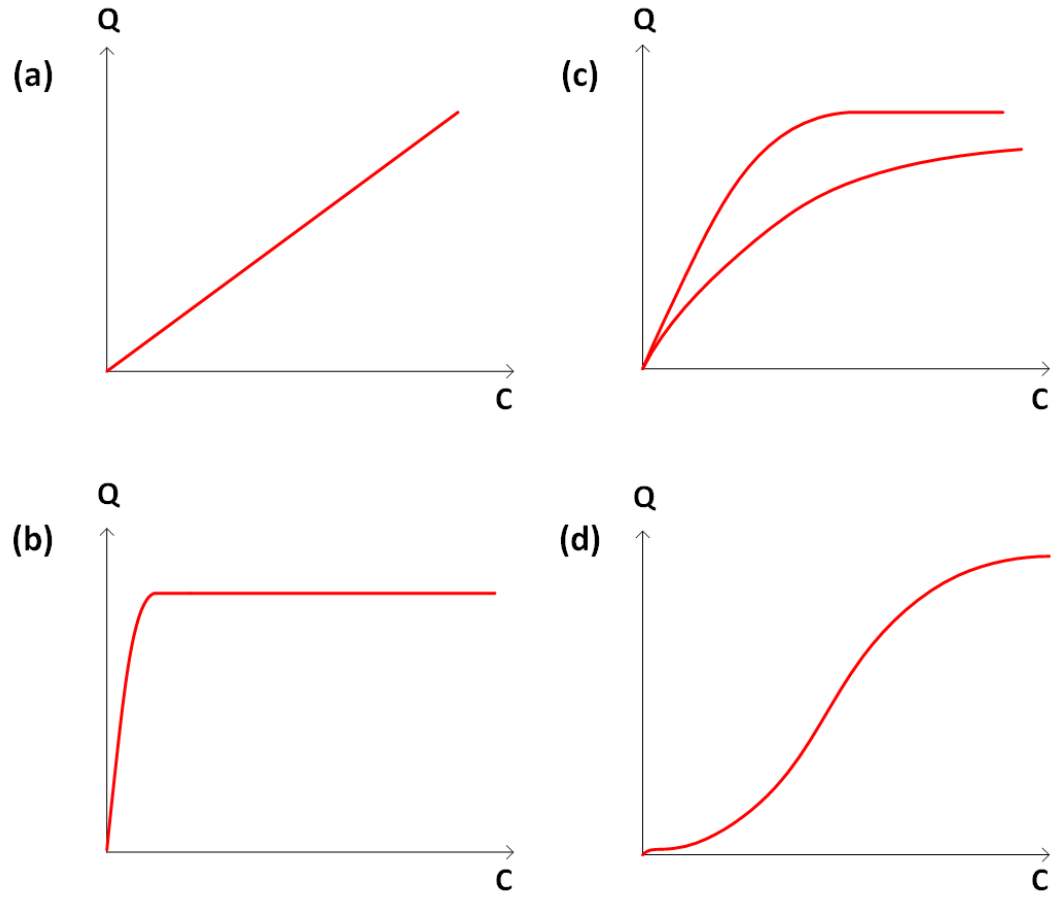

Figure 2-9:different types of batch adsorption isotherms: (a) C-isotherm, (b) L-isotherm, (c) H-isotherm (d) S-isotherm.

C-isotherm: the ratio between Q and C is constant at any time. This can be interpreted as a non-ionic interaction with hydrophobic molecules such as the adsorption of dye onto hydrophobic fibers.

L-isotherm: this is generally a common isotherm as the rate of the curve decreases as the concentration of the adsorbate increases. This suggests a gradual filling of the adsorbent's monolayers. The presence

of the plateau confirms the monolayer has been formed and the effective surface of the adsorbent is completely covered with each adsorbate. Its capacity can be determined from the height of the plateau.

H-isotherm is a particular isotherm belonging to the L-class isotherm. However, the rate of adsorption is very high at the initial stage, which suggests a high affinity of solute on the solid adsorbents. The early occurrence of plateau suggests a strong adsorption of ionic charged solute molecules on opposite-charged adsorbent surfaces.

S-isotherm: this isotherm has a sigmoidal curve. This type of adsorption displays a mixed behavior as two opposite mechanisms may occur (before and after the inflection point). At the initial stage or incubation stage, the increase in the concentration C has no effect on the adsorption effect onto the adsorbent, usually due to the low affinity to adsorbent surface. Activation energy for adsorption of the solute molecules is concentration-dependent and/or is diminished by positive effects of the solvent or the presence of a second solute molecule in the solution.

In aqueous solution (Mansour *et al.*, 2018), the adsorption process isotherms are described by two well-known isotherms (L and H) which can be mathematically written by Langmuir and Freundlich models.

The Langmuir isotherm reads:

$$Q_e = Q_m \frac{K_L C_e}{1+K_L C_e} \tag{2.4}$$

Where Q_e is the equilibrium amount of solute per adsorbent (mg/g), C_e is the equilibrium concentration of the solute, Q_m is the maximum solute concentration per adsorbent. K_L is the Langmuir constant which is related to the adsorption energy and the solution temperature. Q_e is given by the following expression:

$$Q_e = \frac{C_0 - C_e}{m_{ad}} V \tag{2.5}$$

C_0 is the initial concentration, m_{ad} is adsorbent mass, and V is the volume of the aqueous solution.

The Freundlich model reads:

$$Q_e = K_F C_e^{1/n} \tag{2.6}$$

Where K_F is the Freundlich constant, which as K_L is related to the adsorption capacity, energy and the temperature n is a coefficient dependent on the materials. To process the adsorption data, the linearized form can be used:

$$Log(Q_e) = \frac{1}{n} Log(C_e) + Log(K_F) \tag{2.7}$$

In this form, n and K_F can be determined by the slope and intercept of the curve. Typical value of n in the range of 2-10 indicates ideal adsorption behavior.

2.5.2 Mathematical model of adsorption kinetics

The adsorption kinetics provides a link between adsorption capacity and contact time, *t*, in case of aqueous solution. From the kinetics we can obtain different properties such as adsorption rate, dynamic equilibrium, mass transfer, and diffusion rates (Mansour *et al.*, 2018, Sh. Gohr *et al.*, 2022). The examination of these features may give some insights to the comprehension of the adsorption process and its mechanism. To describe the adsorption rates, the experimental adsorption results are fitted using pseudo-first and second order reaction models, as well as an intraparticle diffusion model (Sh. Gohr *et al.*, 2022, Weber Walter and Morris, 1963).

The pseudo-first order reaction model generally assumes very low absorbate uptake, Q_t, this comes from the assumption of monolayer with no interaction given by Langmuir. The differential form of the rate is given by the following expression:

$$\frac{dQ_t}{dt} = K_1(Q_e - Q_t) \tag{2.8}$$

Where K_1 is the kinetic constant (1/min, 1/s or Hz) depending on the activation energy and temperature. The Q_e is the equilibrium or maximum absorbate capacity. The integration of this equation is given in:

$$Q_t = Q_e\big(1 - exp(-K_1 t)\big) \tag{2.9}$$

Another linear form of the pseudo-first order kinetic model is used to interpret the kinetic data, which is given below(Campos *et al.*, 2018):

$$log(Q_e - Q_t) = log(Q_e) - K_1 t \tag{2.10}$$

The pseudo-second order kinetic model assumes a strong interaction (reaction) between the adsorbate and sorbent molecules. The differential and integral expression of the second order kinetic model is given by:

$$\frac{dQ_t}{dt} = K_2(Q_e - Q_t)^2 \tag{2.11}$$

$$\frac{t}{Q_t} = \frac{1}{K_3 Q_e} + \frac{t}{Q_e} \tag{2.12}$$

Where K_2 is the kinetic constant with the unit (g/min/mg) and K_3 in (1/min).

Other types of kinetic models such as diffusion model can be used to fit adsorption kinetics data (Sh. Gohr *et al.*, 2022, Weber Walter and Morris, 1963). This model assumes the diffusion of absorbate particle into a fully formed multilayer or capillary tube of adsorbates.

The kinetic model is given below:

$$Q_t = K_4 t^{1/2} \quad (2.13)$$

The rate constant K_4 is in mg/(g $min^{0.5}$)

2.5.3 Adsorption thermodynamics

Thermodynamics studies the effect of temperature on the adsorption mechanism. Therefore, adsorption is performed at different temperatures (three or more), and the equilibrium constant is plotted as a function of temperature. The spontaneity of an adsorption process as a function of a temperature is assessed by the Gibbs free energy:

$$\Delta G^0 = -RTlogK_D \quad (2.14)$$

Where K_D is the equilibrium constant, R is the universal gas constant, 8.314 J/mol K. The free energy is related to the adsorption enthalpy change, ΔH^0 and the entropy change ΔS^0.

$$\Delta G^0 = -RTlogK_D = \Delta H^0 - T\Delta S^0 \quad (2.15)$$

The Van't Hoff plot that depicts the equilibrium constant versus the temperature $1/T$ allows to determine the enthalpy of adsorption (slope) and the entropy change (intercept) as described by the following equation (Sh. Gohr *et al.*, 2022, Zeng *et al.*, 2023):

$$logK_D = -\frac{\Delta H^0}{RT} + \frac{\Delta S^0}{R} \quad (2.16)$$

2.6 Performance of hydrochar-based activated carbon in heavy metal removal.

Industries like textiles, pulp and paper, and others, release two most hazardous compounds such as heavy metals and dyes into the environment, which can seriously impact water quality. Heavy metals are difficult to remove due to their recalcitrant nature to degradation, posing environmental and health risks as they are toxic and harmful even at low concentrations (> 70 µg/L, See **Table 1**: (Mariana *et al.*, 2021)).

Various technologies exist for heavy metal removal, including coagulation, electrocoagulation, flocculation, adsorption, ion exchange, and more. However, many of these methods are ineffective, expensive, time-consuming, or not versatile for various heavy metals wastewaters. Among these methods, adsorption using activated carbons is considered the most efficient due to its ease of use, flexibility, and simplicity of design. activated carbons are commonly used to remove organic compounds from wastewater because of their excellent adsorption properties (Ioannidou and Zabaniotou, 2007). However, their widespread use is limited by the high production and regeneration costs. To make adsorption treatment more cost-effective, researchers are exploring the use of cheap and readily available materials. Wastewater sludges and biomass, often waste from industrial and agricultural processes, are considered promising precursors for creating low-cost and efficient

adsorbents due to their abundance and affordability. Thermochemical conversion of such liquid wastes using hydrothermal carbonization results in a low-cost carbon-rich materials called hydrochar (Koprivica *et al.*, 2023).

Prior research has demonstrated the feasibility of utilizing hydrochar-derived activated carbon for the removal of heavy metals from water and wastewater. These studies have investigated the adsorption efficiency, surface properties, and regeneration potential of hydrochar-derived activated carbon (Ighalo *et al.*, 2022). However, there is a need for further research to explore the applicability of this sustainable material specifically for the removal of heavy metals, as well as to conduct comprehensive sustainability assessments. Anirudham and Sreekumari (Anirudhan and Sreekumari, 2011) performed a batch adsorption process to investigate activated carbon (AC) derived from waste coconut buttons (CB) as a suitable adsorbent for the removal of heavy metal ions such as Pb(II), Hg(II), and Cu(II) from industrial effluents. Elemental analysis, Fourier transform infrared spectroscopy, X-ray diffraction, scanning electron microscopy, thermal gravimetric and differential thermal analysis, surface area analyzer, and potentiometric titrations were used to characterize the AC. The effects of initial metal concentration, contact time, pH, and adsorbent dose on metal ion adsorption were investigated. The adsorbent demonstrated good adsorption potential for Pb (II), Cu(II), and Hg(II) at pH 6.0 and 7.0, respectively. (Acharya *et al.*, 2009) demonstrated that Tamarind wood-activated carbon is an effective adsorbent for removing lead (II) from aqueous solutions. Characterization revealed a distinct difference in the physicochemical properties of the adsorbent. According to the kinetics studies, lead (II) adsorption is very fast in the beginning and slows down as it approaches equilibrium. The equilibrium time increases as the initial concentration of lead (II) increases. The percentage removal of lead (II) increases as the adsorbent dosage increases and decreases as the initial lead (II) concentration increases. The experimental results agree well with the Langmuir adsorption isotherm model and have a better fit for the experimental data. Lead (II) adsorption follows a pseudo-second-order equation with good correlation. Zhou *et al.* (Zhou *et al.*, 2017) investigated the Pb (II) adsorptive ability of biochars based on fresh and dehydrated banana peels obtained by an one-step hydrothermal carbonization process, using 20% phosphoric acid as the reaction medium. The resulting biochars had an oxygen content of about 20% and were rich in surface functional groups like hydroxyl and carboxyl, significantly boosting their adsorption capabilities. These sorbents demonstrated impressive lead removal capacities, with 359 $mg \cdot g^{-1}$ for dehydrated banana peel biochar and 193 $mg \cdot g^{-1}$ for fresh banana peel biochar. The analysis indicated that ion exchange was the primary mechanism behind lead removal, as evidenced by changes in chemical bonds on the surface. The study by (Nzediegwu *et al.*, 2021)investigated the lead(II) adsorption mechanisms using biochars produced through microwave-assisted pyrolysis and hydrochars created via hydrothermal carbonization at different temperatures using various feedstocks. The showed that the highest lead (II) adsorption capacity (165 mg g^{-1}) was achieved with biochar derived from canola straw at 500°C. Moreover, biochars generally outperformed hydrochars in lead(II) adsorption,

except for chars made from sawdust. This difference was attributed to variations in solution pH influenced by char pH. Additionally, lead (II) adsorption decreased in hydrochar as the production temperature increased, mainly due to interactions with aromatic carbon. In contrast, lead (II) adsorption increased in biochar due to precipitation as hydrocerussite and lead oxide phosphate. (Wang *et al.*, 2020) synthesized hydrochars based on a mixture of honey and deionized water using a hydrothermally carbonization at 180 ℃. It was observed that the obtained hydrochar was rich in carbon-oxygen functional groups. The maximum adsorption capacity of lead was 133.2 $mg \cdot g^{-1}$ at a pH = 5 and temperature = 25 ℃. (Guo *et al.*, 2019) prepared activated carbons from a mixture of urea/$ZnCl_2$ and ground branch wastes of Camellia sinensis. The mixture was then hydrothermally carbonized in a batch reactor at 240 ℃. The hydrochar's surface consisted of 45.52% graphitic nitrogen with a surface area of 63.1 m^2/g and pore diameter of 18.35 nm. The batch adsorption experiments depicted a 143.88 $mg \cdot g^{-1}$ adsorptive capacity of lead ions at a temperature = 60 ℃ and pH = 5.0. Luo *et al.*(Luo *et al.*, 2020)synthesized hydrochars from a blend of sewage sludge conditioner solution containing magnesium nitrate, urea, and aluminum nitrate. The hydrothermal carbonization was performed at 120 ℃. It was found that the hydrochar has a flocculent or lamella structure with rough surface and was rich in oxygen and nitrogen containing functional groups. The maximum adsorption capacity of Pb (II) was 62.44 $mg \cdot g^{-1}$ at temperature = 25 ℃: pH = 4.3. The mechanisms of adsorption were physisorption of Pb (II) into the porous structure of the hydrochar through van der Waals force, electrostatic attraction, and ion exchange between Pb (II) and –COO, -C-N, and N-C-O on the hydrochar.

2.7 Research Gaps and Contributions

While the literature provides valuable insights into the potential of hydrochar-derived activated carbon, there is a lack of studies investigating the adsorption performance of hydrochar derived from wastewater sludges. Furthermore, there remains a gap in the understanding of its performance in removing heavy metals from wastewater effluent. This thesis seeks to bridge this gap by conducting a systematic investigation into the adsorption capacity, structural characteristics, and sustainability aspects of hydrochar-derived activated carbon in the context of heavy metals removal. By addressing this research gap, the study aims to contribute to the development of environmentally friendly and effective solutions for the treatment of wastewater and the protection of water resources.

Continued research and development in this field hold the promise of advancing sustainable wastewater treatment practices and mitigating the environmental and health risks associated with micropollutants in wastewater effluent. In the subsequent chapters, we will delve into the methodology, experimental results, and discussions that constitute the core of this investigation.

3 MATERIALS AND METHODS

This chapter discusses two parts; the first part describes materials and methods utilized towards the preparation and characterization of the activated carbon as a potential absorbent. In the second part, the preparation of stock solutions of lead (II) ($Pb^{2+)}$ are developed. Then, a description of batch methods for kinetic and equilibrium studies of Pb^{2+} adsorption on prior activated carbon is given. These studies are crucial to assess the efficacy of the hydrochar-derived activated carbon in removing Pb^{2+} ions from solution.

3.1 Preparation and characterization of the activated carbon

3.1.1 Preparation

In this work, the performance of two types of activated carbons in removing Pb^{2+} was investigated: (i) a commercial activated carbon, GAC (granular activated carbon), and (ii) one prepared in our laboratory named HC425 (Hydrochar annealed at 425°C). The procedure of HC425 preparation is similar to that described by (Facchin et al., 2023). The process involves annealing of hydrochar in a tubular furnace (See Figure 1) at a temperature determined by the TGA (Thermogravimetric analysis).

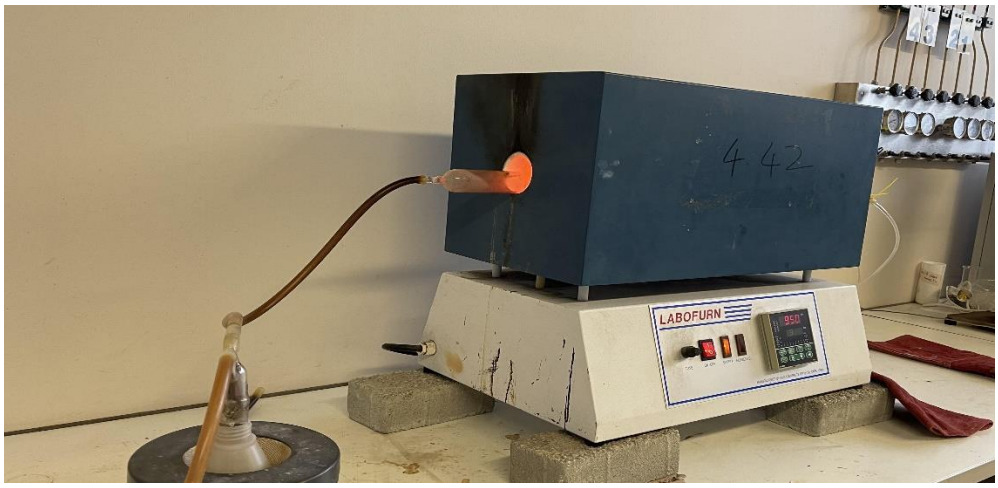

Figure 3-1: Muffle furnace (Annealing procedure)

Two stages are involved in the annealing process. To stabilize the temperature and dry out the hydrochar, the furnace is first heated from room temperature (25 ℃) to 100 ℃ at a rate of 10 ℃/min. Secondly the furnace is heated at a rate of 20 °C/min from 100 °C to the predetermined final temperature of 425 ℃, maintained there for 60 minutes, and then cooled to 200 °C at a rate of 20 °C/min before being naturally cooled to room temperature. Throughout the entire experiment, an inert gas (N_2) is passed through the furnace at 1.0 ml/min to prevent any unintended combustion or gasification. Before

and after the annealing process, hydrochar is weighed. For additional analyses, hydrochar is kept in a desiccator and stored in a centrifuge tube (Saha *et al.*, 2019).

3.1.2 Characterization

Usually, the characterization of the prepared activated carbon should provide information on: (1) its chemical composition; (2) its ability to sorb and retain molecules; (3) its structure and morphology. The characteristics of activated carbon can be described using the following parameters: (i) iodine number, (ii) pH at the point of zero charge, (iii) bulk density, (iv) Ash content, (v) moisture content, (vi) SEM (Scanning electronic microscopy) images, (vii) surface area, (viii) particle size, and (ix) complex attachments to the activated carbon using Fourier Transform Infrared spectroscopy. The methods used towards measurement of these parameters are described below.

Iodine number: When the iodine equilibrium concentration is 0.01M, the iodine number is defined as the milligrams of iodine (I_2) adsorbed by 1 g of activated carbon. The three-point method (Haimour and Emeish, 2006) was used in this project for three different temperatures (250, 350 and 450 °C). The following steps are used to determine the iodine number: Three dry samples of activated carbon, weighing between 300 and 600 mg each, were divided among three 250-ml conical flasks. Each flask received ten milliliters of a 5% (by weight) hydrochloric acid solution before being mixed until the carbon was moist. The mixtures were then brought to a boil for 30 seconds before being cooled. Each flask received 100 milliliters of 0.05M standard iodine solution. After 30 seconds of vigorous shaking, the contents were immediately filtered. Each filtrate was titrated with a 50 ml aliquot of a standard 0.1M sodium thiosulfate solution. The obtained iodine residual concentration for each sample should be divided into 0.004 and 0.02 M. A straight line is produced when the amount of iodine fixed per gram of sorbent is plotted against the residual iodine concentration, allowing the iodine number to be graphically determined (ordinate corresponding to a residual concentration of 0.01M).

pH at the point of zero charge (Nasiruddin Khan and Sarwar, 2007), The Point of Zero Charge (pzc) is the pH of the aqueous solution at which the solid exhibits a neutral electric potential—specifically, the pH at which the initial value and the final value are identical (i.e., the pH at which the electric charge density of a given surface equals zero). It enables measurement of carbon's acidic or essential nature. Activated carbons can have an acidic, basic, or neutral nature depending on the precursor origin and the preparation method (chemical or physical). The carbon surface is positively charged at pH < pHpzc and negatively charged at pH > pHpzc. The method outlined by (Nasiruddin and Sarwar ,et al,2007)was used to determine pHpzc. The steps of this method involve: (1)Weigh 5.0 g air-dried Biochar sample (ground to <2 mm) into a 100 mL centrifuge tube or bottle. (2) Add 50 mL deionized water (DIW) using an automatic dispenser, close the lid and shake well by hand. (3) Mechanically shake for 1 h at

25°C and allow the suspension to stand for ~30 min. (4) Measure the suspension pH using a pH meter calibrated pH 7 and pH 10 buffers. If the expected pH of the Biochar is <7, then use pH 7 and pH 4 buffers for calibration. (5) Record the pH value after stabilization. Rinse electrodes (with deionized water) and blot dry between measurements.

Bulk-density: Into a dry graduated cylinder of 250 ml (readable to 2 ml), gently introduce, without compacting, approximately 20, 50, 80 and 100 g of the test sample (m) weighed with 0.1% accuracy. Carefully level the powder without compacting, if necessary, and read the unsettled apparent volume (V_0) for each mass, to the nearest graduated unit. The calculated density would be the slope of linear curve of m = f (V_0).

Ash content %: Ignite crucible in muffle furnace at 650℃± 25℃for 1 h. Place crucible in the desiccator. Cool to room temperature and weigh to the nearest 0.1mg. Weigh out to the nearest 0.1 mg sufficient dried activated carbon so that the estimated amount of ash will be 0.1 grams into the ignited crucible. Then place the crucible in the furnace at 650 ℃± 25℃. Note that, ash formation will take place from 3-16 hours depending on the type of activated carbon and its particle size. Ash forming can be considered complete when constant weight is achieved. Finally, place the crucible in the desiccator and allow it to cool to room temperature. When cool admit air slowly to avoid loss of ash from the crucible. Weigh to the nearest 0.1 mg. Ash content Ac is given in % by the formula below:

$$Ac = 100\frac{F-G}{B-G} \tag{3.1}$$

Where, G= mass of empty crucible; B = mass of crucible plus dried sample g; F= mass of crucible plus ashed sample in

Moisture content (%): The moisture content is determined by thermogravimetry analysis (TGA). This is done by measuring the weight loss during the heating of Activated carbon from room temperature (25 ℃) to 150 ℃ for 2 -3 hours in an oven.

SEM (Scanning electronic microscopy): The surface morphology, topography of the commercial and prepared activated carbons was investigated using a ZEISS EVO50 scanning electron microscope. The samples were prepared by spreading dried carbon powder onto 10 mm aluminum stubs, using double-sided glued carbon discs, and then placing them in a vacuum sample chamber. The stub is sputter coated with gold palladium alloy or carbon. Images were taken under high vacuum condition using the secondary electron detector.

Surface area (m^2/g): The total surface area can be determined by Brunauer–Emmett–Teller (BET) analysis. The BET surface area is calculated from N_2 adsorption isotherms at 77 (K) by using the BET equation (Brunauer *et al.*, 1938) (see Eq. (2.3) in Chapter 2).

Particle size (µm): For this, we use sieving method. It is the most traditional method to separate solid powders into defined proportions of specified particle size. In doing so, the powder of Activated Carbon is sieved through a stack of sieves with decreasing mesh size (top to bottom) and simultaneously shaken for a period of time (10-20 minutes). After the separation, Activated Carbon with different particle size settle in each sieve which are weighed to find the particle size distribution.

Fourier Transform Infrared spectroscopy (FTIR)(Fu et al., 2022): The FTIR from PerkinElmer single reflection diamond module was used for analyzing all the complex attached to the prepared activated carbon. The sample platform and the stub were cleaned properly before and after each run using ethanol. The amount 10-15 mg of prepared samples were placed onto the diamond crystal surface. Finally, a force was applied to the sample for spectrum collection. The sample was then removed from the crystal surface and cleaned again in order to prepare the accessory to collect additional spectra.

3.2 Heavy metal (Pb^{2+}) removal

All the chemicals used were of analytical reagent grade. Lead nitrate salts were used for synthesis of stock solutions. The stock solution's pH was adjusted using Hydrochloric acid and Sodium hydroxide. Deionized water was used throughout the experimental studies.

Figure 3.2 depicts the experimental procedure employed for the Pb^{2+} removal. At the beginning, two simultaneous tasks are conducted. On the one hand, the activated carbons synthesized and characterized according to the procedure elaborated in previous subsections. On the other hand, stock solution and different batches with different initial concentrations are made just by diluting the stock solution with different amount of water. Then follows a parameter analysis to find the optimal parameters to the Pb^{2+} removal efficiency. Once the optimal operating conditions have been determined, adsorption kinetics and isotherms are conducted.

3.2.1 Stock solution preparation

In order to simulate a lead-containing wastewater, aqueous solutions of Pb^{2+} ions was prepared by dissolving lead (II) nitrate ($Pb(NO_3)_2$) in deionized water. Initially, a stock solution of 500 mg/L of Pb(II) ion is prepared by dissolving ~0.8 g of lead(II) nitrate in 1000 mL of deionized water. The subsequent preparation of solution with multiple Pb^{2+} concentrations of 2.5, 5, 10, 15, 20 mgL^{-1}, and so on is made by diluting the stock solution with deionized water.

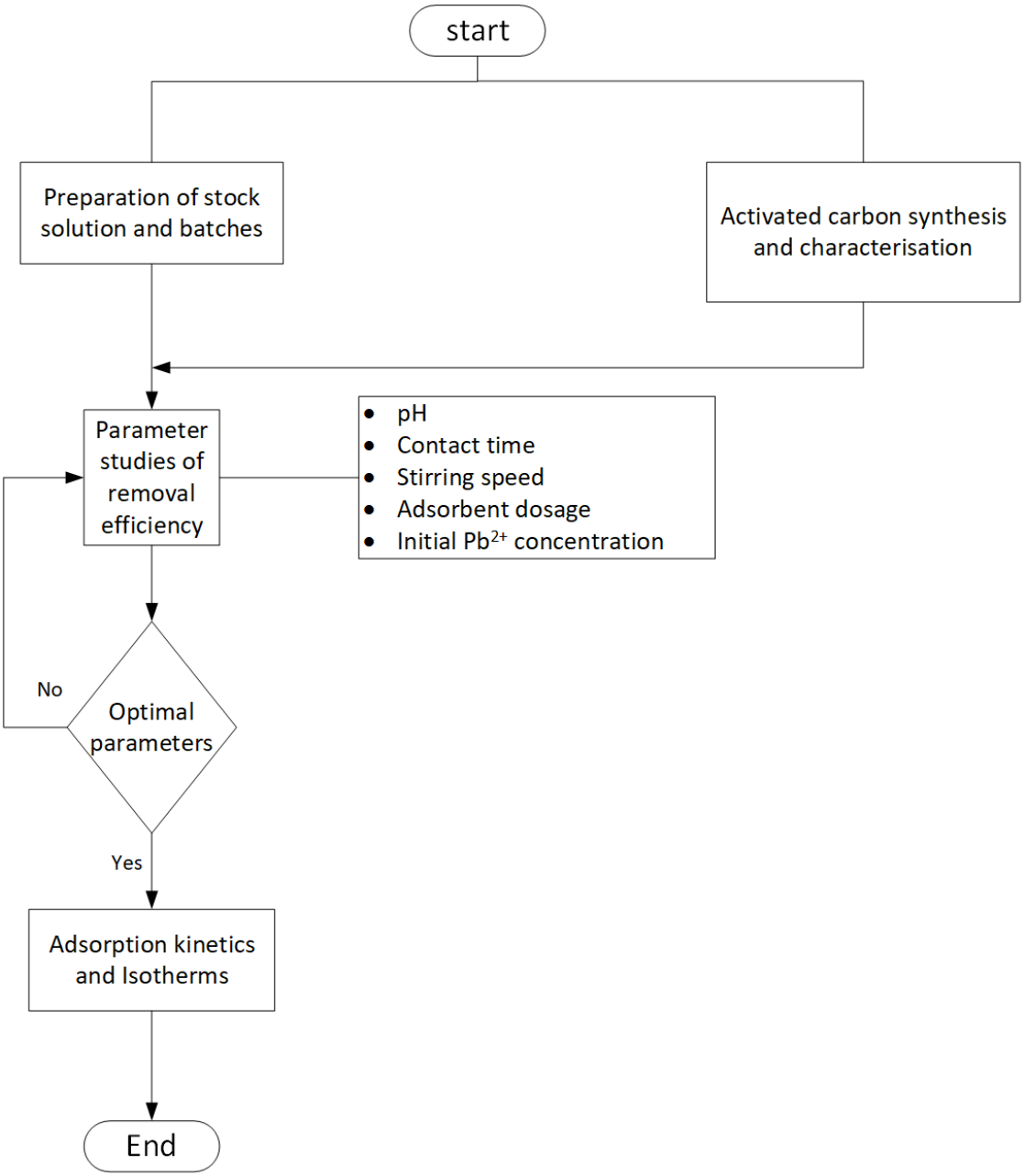

Figure 3-2: Flowchart of the experimental protocol of batch adsorption

3.2.2 Adsorption experiments

Batch adsorption experiments of lead (II) were carried out to determine the adsorption capacity of prepared activated carbons (AC) at different metal concentrations ranging from 2.5 to 20 mg/L and a fixed amount of AC in order to calculate the adsorption constant using different isotherms. In doing so, the effects of varying (1) the solution pH, (2) the adsorbent dosage, (3) the initial lead (II) ion concentration and (4) the contact time, on the isotherms were investigated.

First, with all the other parameters (Pb^{2+} concentration, AC dosage and contact time) fixed, hydrochloric acid (HCl) and Sodium hydroxide (NaOH) were used to adjust the solution pH. Deionized water was

used throughout the experimental studies. Once the optimum pH was found, then the effects of varying the AC dosage from 0.1 to 0.5 g with an increment of 0.1g on the adsorption performance were conducted, while other parameters are fixed. For this purpose, these five different masses of AC were put in 100 ml of stock solutions. The blend was shaken at 150 rpm for 120 minutes. The effect of the initial Pb^{2+} concentration on the efficiency of AC in the removal of heavy metals from the solution was determined using solution concentrations in the range of (2.5, 5, 10 and 20) mg/l. Thus, 100ml of the solution samples were in contact with previously optimized AC dosage at an agitation speed of 150 rpm for 120 minutes. The pH of the solution was adjusted to the optimal one. For each experiment conducted, samples were collected every 15 mins. The initial and timely-collected concentrations of the solutions were measured by Inductively Coupled Plasma-Optical Emission Spectrometers (ICP-OES). After equilibrium was attained, the metal adsorption capacity for each sample was calculated according to:

$$q_e = \frac{C_0 - C_e}{m} V \qquad (3.2)$$

Where m is the mass of AC (g), V is the volume of the solution (L), C_0 is the initial concentration of lead (II) (mgL-1), C_e is the equilibrium lead (II) ion concentration (mgL-1) and q_e is the Pb^{2+} weight capacity adsorbed at equilibrium (mg/g). The removal percentage of Pb^{2+} from the solution was calculated by the following equation.

$$R\% = \frac{C_0 - C_e}{C_0} \times 100 \qquad (3.3)$$

Where C_0 (mg/L) is the initial metal ion concentration and C_e (mg/L) is the final Pb^{2+} concentration in the solution.

3.2.3 Adsorption isotherms

To study the interaction between adsorbate (Pb^{2+}) and adsorbent (AC), isotherm curves are required(Ashfaq *et al*., 2021, Misran *et al.*, 2022). These curves are portrayed by plotting the solid phase concentration q_e versus the liquid phase concentration C_e. The Langmuir and Freundlich isotherms are the most widely utilized models to describe batch adsorption experimental data. In the present work, these two isotherms were applied to investigate the adsorption process of Pb (II) on prepared AC at different process parameters.

Langmuir isotherm model: The Langmuir adsorption is usually the simplest and best model among the span of isotherms models, and it has been successfully applied in many adsorption processes. The Langmuir isotherm model generally assumes sorption of monolayer of adsorbate onto

an adsorbent surface with a finite statistical number of identical sites with equal site energy. The linearized Langmuir equation is written as (Sh. Gohr *et al*., 2022):

$$\frac{C_e}{q_e} = \frac{1}{K_L q_m} + \frac{C_e}{q_e} \tag{3.4}$$

Where C_e, and q_e were previously defined, q_m is the maximum adsorption capacity (mg/g) and K_L is the Langmuir constant related to the relative energy of adsorption (1/mg).

Freundlich isotherm model: Freundlich isotherm model is also one of the most increasingly used mathematical models which fit the experimental data over a wide range of concentration. This model assumes that the adsorbent surface are heterogeneous which leads to a distribution of active sites with different adsorption energy. The linearized Freundlich equation reads (Sh. Gohr *et al.*, 2022):

$$Log(q_e) = \frac{1}{n} Log(C_e) + Log(K_F) \tag{3.5}$$

Where K_F and n are Freundlich equilibrium constants.

3.2.4 Adsorption kinetics

The kinetic study of adsorption in wastewater is significant because it provides crucial insight into the reaction pathways and mechanism The mechanism of a solute sorption from an aqueous solution onto an adsorbent has been explained by the following kinetic models(Misran *et al*., 2022): (1) Pseudo- first order kinetic model, (2) Pseudo-second order kinetic model

Metal adsorption kinetics have been predicted using the pseudo first-order kinetic model for a long time. According to the pseudo first-order model, the metal adsorption kinetics are given by (Ho and McKay, 1999a):

$$log_{10}(q_e - q_t) = log_{10}(q_e) - \frac{K_1}{2.302} t \tag{3.6}$$

Where K_1 (min^{-1}) is the rate constant of the pseudo-first-order adsorption, q_t (mg/g) denotes the amount of adsorption at time t (min) and q_e (mg/g) is the amount of adsorption at equilibrium. Using Ho's pseudo-second-order kinetics, the adsorption kinetic data may be examined in more detail (Ho and Mckay, 1999b)

$$\frac{t}{q_t} = \frac{1}{K_2 {q_e}^2} + \frac{t}{q_e} \tag{3.7}$$

Where K_2 (g/(mg min)) is the rate constant, K_2 and q_e can be obtained from the intercept and slope.

4 RESULTS AND DISCUSSION

The present chapter investigates the performance of lead (II) ions adsorption. First, the results of preparing the activated carbon based on hydrochar are presented. Then, the prepared adsorbents are characterized by the well-known techniques introduced in the previous chapter. Next, the effects of the influencing parameters such as solution pH, adsorbent dosage, lead (II) ions concentration, contact time, and lead(II) ions removal efficiency are discussed. Finally, the equilibrium and the kinetic mechanism of lead (II) ions on the prepared activated carbon are discussed.

4.1 Preparation and characterization of the activated carbons

4.1.1 Preparation

A thermogravimetric analysis was conducted on the hydrochar derived from a combination of primary sludge and waste-activated sludge (referred to as HC-PS-WAS-Scr), which serves as the precursor for hydrochar-derived activated carbon (HC-AC). The purpose of this analysis was to evaluate the thermal stability of HC-PS-WAS-Scr and identify the optimal pyrolysis temperature for achieving a significant carbon yield. **Figure 4.1** below illustrates the thermogram of the composite material consisting of primary sludge (PS), waste-activated sludge (WAS), and screenings.

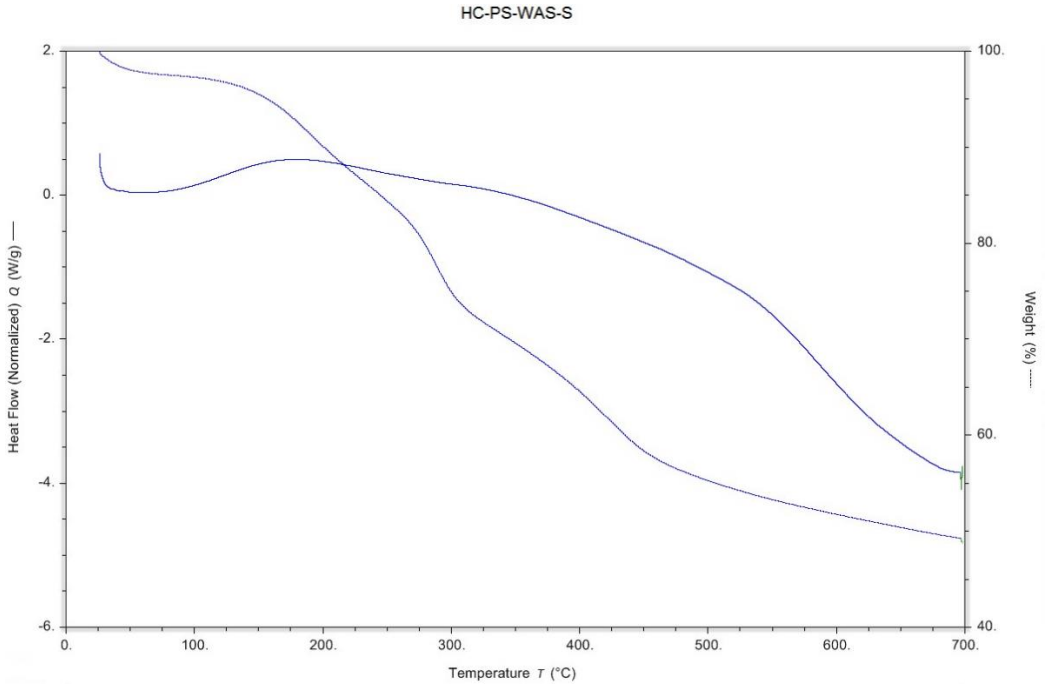

Figure 4-1:Thermogravimetric analysis of HC _PS_WAS_Scr

The temporal derivative mass curve in **Figure 4.1** exhibits three discernible stages. The initial stage spans from 25°C to 225°C, characterized by a significant decrease. This is followed by a sharp decline occurring between 275°C and 450°C. Subsequently, a moderate decrease is observed from 450°C onwards, with the curve stabilizing around 700°C. The first temperature range, spanning from 25°C to

225°C, exhibits a weight reduction of approximately 5.5%. This phenomenon can be attributed to the liberation of moisture and volatile substances. On the other hand, the significant and abrupt weight decrease of roughly 35% occurring between 275°C and 450°C is ascribed to the degradation of proteins and polymers with low molecular weight. The third and final step exhibited a weight reduction of approximately 2.5%, which persisted until reaching a temperature of 700°C (De Filippis et al., 2013).

Two temperatures were selected and examined for activated carbon production, as indicated by the TGA curve in **Figure 4.1**. The percentage weight loss and yield results were determined by applying Eq.(3.1) from the previous chapter. The outcomes that were obtained are presented in **Table 4.1**. Furthermore, **Figure 4.2** shows a photograph of the weight loss during the pyrolysis procedure.

Table 4-1:Percentage of weight loss and yield

Pyrolysis Temp	**350**°C	**450°C**
Weight loss(%)	20.1	54.9
Yield %	77.5	65.7

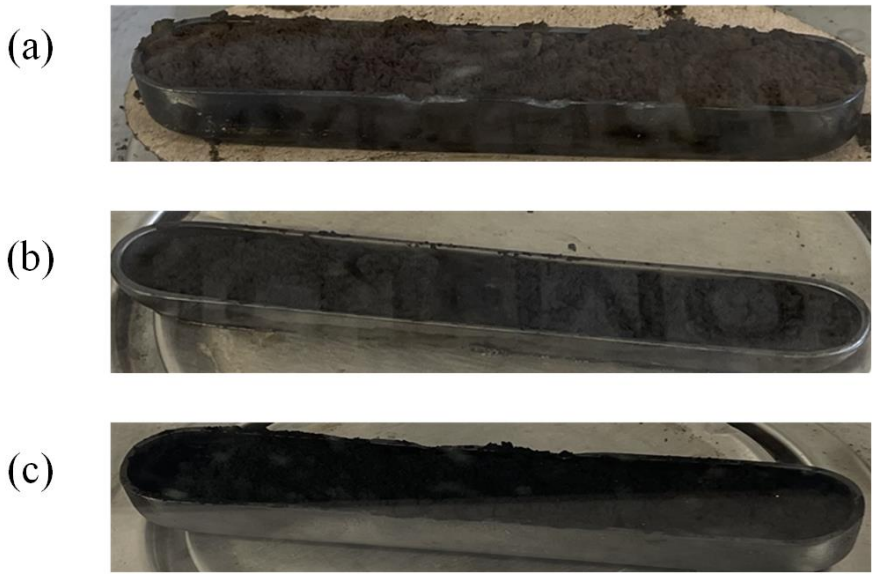

Figure 4-2: (a) HC-PS-WAS-Scr, (b) HC-PS-WAS-Scr (350°C), (c) HC-PS-WAS-Scr (450°C)

Of the two temperatures, the pyrolyzed product at 450°C had the lowest carbon yield (65.7%) and showed signs of ashing. As a result, it was excluded from any further investigation. Though the pyrolyzed product at 350°C had a high carbon yield (77.5%) when compared to that at 450°C (65.7%), the product resulting from pyrolysis at 450°C was chosen as the best and the one to be used for the adsorption tests as it had a higher iodine number (86.165 mg/g). As we advance, the pyrolyzed product

at 450°C is referred to as hydrochar-derived activated carbon (HC-PS-WAS-Scr)(de Caprariis et al., 2017) and Similar results were obtained .

4.1.2 Characterization of Activated Carbon

Before conducting the adsorption studies, the two activated carbons (GAC and HC-PS-WAS-Scre) underwent characterization tests to determine various properties. These properties include moisture content, ash content, surface area, bulk density, particle size, pH, chemical composition, surface morphology, iodine number, functional groups, and particle size. The methods used for determining these properties were outlined in the experimental details. **Table 4.2** summarizes the list of characterization techniques employed on the prepared activated carbon. Its performance was compared with a commercial granular activated carbon (GAC).

Table 4-2: Characterization tests performed on commercial GAC and HC-PS-WAS

Parameters	**GAC**	**HC-PS-WAS- Scr**
pH	8.79	3.21
Attrition (%)	46	76
Ash Content (%)	2.9	69.8
Moisture Content (%)	4.01	1.49
Bulk density (kg/m^3)	490	320
Particle size (µm)	425-2,360	79-180
Iodine Number (mg/g)	1201.03	86.165

- *pH*

The pH of the adsorbents was determined, revealing that GAC had the highest pH value of 8.79, while HC-PS-WAS-Scr had a pH of 3.21. The majority of activated carbons mentioned in the literature have alkaline pH values due to the use of deionized water for washing after activation and carbonization, which helps to neutralize the pH(WAJI, 2018)(Weng,et al 2014). The exceptionally low pH of HC-PS-WAS-Scr can be ascribed to the absence of a washing step following carbonization.

- *Attrition*

When selecting granular adsorbents for wastewater treatment, resistance to attrition is a significant parameter to consider(Wuana, et al 2015). This parameter provides valuable information regarding the mechanical strength of the carbon and its ability to withstand disintegration during transportation, regular handling, and regeneration(Alcañiz-Monge et al., 2022, Kale, 2019). The potential for intraparticle abrasion is significant in granular carbons due to their properties and applications(Toles et

al., 2000). This can result in the formation of fine particles with low abrasion resistance (high losses), potentially causing system blockages(Mudhoo et al., 2023). The attrition test was exclusively conducted on GAC and AW-AC due to the refined nature of the particles of HC-PS-WAS-Scr, which are typically in powdered form, making it challenging to determine loss through attrition accurately. The findings presented in **Table 4.2** indicate that GAC demonstrates a comparatively lower resistance to attrition (32%), in contrast to HC-PA-WAS-Scr (76%). The outcome of HC-PS-WASP-Scr indicates carbons obtained from biomass rich in cellulose, which is brittle by nature(Jjagwe et al., 2021) and consequently has a more excellent attrition value. This finding provides further evidence in favor of the hypothesis that the attrition resistance of carbon is directly influenced by its precursor(Sugumaran et al., 2012). The findings of this research further corroborate the assertion made by (Toles et al., 2000) that a correlation exists between attrition and density, wherein carbons with reduced density generally demonstrate increased attrition. This phenomenon is illustrated with HC-PS-WAS-Scr, which exhibits a greater attrition value of 76% in contrast to the 46% recorded for GAC, and a lower bulk density of 0,32g/cm3 in comparison to GAC (0.49 g/ cm^3).

- *Ash content and surface area*

In contrast to HC-PS-WAS-Scr, which possesses a substantial surface area of 115.21 m^2/g and a high ash content of 69.8%, GAC, and HC-PS-WAS-Scr exhibit notably reduced ash contents of 2.9% and 69.8%, respectively, in addition to a substantial surface area of 1055 and 115.21 m^2/g. In the literature, the relationship between high ash content and low surface area has been extensively debated, with the primary cause being the occlusion of pores by the ash(Ma et al., 2013, Everson et al., 2008, Ahmaruzzaman, 2010). The HC-PS-WAS-Scr values obtained in this research exhibit a relatively high ash content, which is similar to the values documented in the literature regarding adsorbents derived from sludge (Almahbashi et al., 2021, Mkungunugwa et al., 2021). The correlation between high ash content and low carbon content was also documented, and this is corroborated by the EDS spectrum data presented further down in this chapter.

- *Moisture content (%)*

Moisture content was found to be the lowest in GAC and HC-PS-WAS-Scr, which were the two activated carbons (4.01 and 1.49%, respectively). Activated carbons derived from lignocellulosic materials typically contain the highest moisture content(Köseoğlu and Akmil-Başar, 2015, Cheok, 2013). There is evidence that activated carbons with a high moisture content have a diminished adsorption capacity (Vasiraja et al., 2023).The moisture content of the two activated carbons is below 8%, which satisfies the American Water Works Association's (AWWA) GAC requirements(BECKER et al., 1974).

- *Bulk density*

An essential parameter for determining the volume capacity of activated carbon, bulk density is typically correlated with the capacity of the carbon to adsorb more adsorbate per unit volume during adsorption(SE et al., 2013, Doyle et al., 2018). The respective bulk densities of GAC and HC-PS-WAS-Scr are 0.490 g/cm^{3}and 0.320 g/cm^3. The practical use of activated carbon is limited to 0.25gm/l, as established by the American Water Works Association(BECKER et al., 1974, Evbuomwan et al., 2013). All three carbons have bulk density values exceeding this threshold, indicating their suitability for wastewater treatment. Carbon bulk density is significantly influenced by the precursor and treatment method employed. It has been reported that the bulk densities of adsorbents derived from woody biomass are greater than those of industrial and municipal solid wastes such as sludge(Jindo et al., 2014). On the contrary, it has been suggested that an adsorbent with a bulk density below 1.2 g/cm^3 possesses a reduced particle size, enhancing its adsorption capacity(Kennedy and Summers, 2015).

- *Particle size*

The particle size of the adsorbents was determined using sieves, following the methodology described in the preceding chapter. A range of sieves with apertures between 425 μm and 2360 μm was employed to ascertain which sieves would exhibit the most significant retention of GAC at a mass of 100g. A combined percentage of 91.6% of the carbon was retained on the 425 μm and 2360 μm sieves; thus, this fraction was utilized in all experiments. The particle size distribution of HC-PS-WAS-Scr was assessed using sieves with a range of 45 to 150μm. 99.8% of the carbon material was retained on the 79 and 180μm sieves, and this fraction was utilized for the experimental analysis.

- *Iodine number*

The iodine number is a method employed to determine the surface area and microporosity of activated carbon accurately; it is also utilized to assess the activation level of an adsorbent(Ahmed and Theydan, 2012). It is defined by the procedure of the American Society for Testing and Materials(D4607-94, 2006) as the quantity of iodine adsorbed per gram of carbon at a 0.02 N residual iodine concentration, expressed in milligrams. **Table 4.2** presents the iodine number values that were acquired for the three adsorbents. The obtained iodine concentrations for HC-PS-WAS-Scr and GAC were 1201.03 mg/g and 86.12 mg/g, respectively. The GAC has an iodine number ranging from 500 mg/g to 1250 mg/g, suggesting a significant level of activation. One may assert that HC-PS-WAS-Scr exhibits minimal activation by employing the identical metric. While the American Society for Testing and Materials (D4607-94, 2006) procedure does not permit generalization of the relationship between the iodine number and surface area, the obtained results corroborate with the BET results that the surface area of the GAC is higher than that of HC-PS-WAS-Scr

- *Raman spectroscopy*

Raman spectra were acquired across a wavelength range of 10-3000 cm^{-1}. The appearance of two discernible peaks on each of the carbon samples is illustrated in Figure 4.3. The GAC and HC-PS-WAS-Scr are carbon samples whose Raman spectra contain 1336 cm^{-1} and 1356 cm^{-1} characteristic bands, respectively. The D band peaks, present in this particular range, emphasize imperfections and disarray within the carbon crystalline structure(Ghosh et al., 2018). At 1595 cm^{-1} and 1586 cm^{-1}, sharp peaks are observed for the GAC and HC-PS-WAS-Scr samples. The peaks observed within this frequency range indicate the G-band, a graphitic arrangement that is the principal signature for sp2 carbon in Raman spectra. a C-C bond in the G-band signifies that sp2 atom pairings are stretched in rings and chains(Chia et al., 2012). Vague second-order Raman spectra exhibited peaks at approximately 2881 and 2662 cm^{-1} for GAC, HC-PS-WAS-Scr, respectively. The peaks falling within this range are known as 2D bands, which indicate that these carbons possess a low level of organization in aromatic regions but have a high concentration of sp3 bonds(Belousov et al., 2022, Orlando et al., 2021). The presence of both D and G bands provides evidence of the carbons chia's polyaromatic and graphitic nature(Chia et al., 2012). Within the context of graphene and carbon materials, the intensity of the D band in the GAC (Graphene and Amorphous Carbon) spectrum is greater than that of the G band. This heightened intensity suggests the presence of a significant amount of disorder in the arrangement of carbon atoms. The D band in AW-AC and HC-AC exhibits lower intensity compared to the G band, indicating a minor level of carbon atom disorder. The degree of disorder in carbon materials is quantified by the ratio of intensities between the D and G bands (R = ID/IG)(Medhat et al., 2021). The intensity ratios of the activated carbons GAC, AW-C, and HC-AC are 0.84, 0.84, and 0.86, respectively. The resemblance of the three numbers indicates that the carbons possess comparable graphitic structures (Katz et al., 2022).

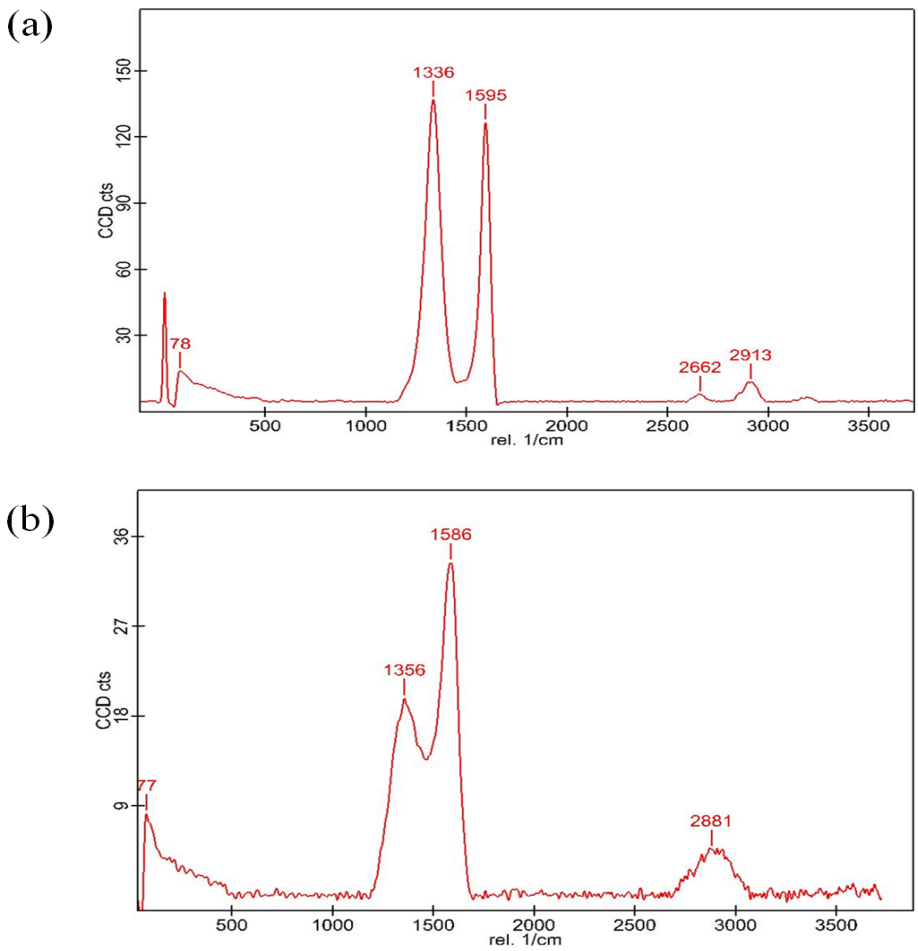

Figure 4-3:Raman spectra of (a) GAC, (b) HC-PS-WAS-Scr

The FTIR (**Figure 4.4**) was used to analyze the surface functional groups of the prepared activated carbon. Fewer functional groups were detected on the surface of the tested samples. For example, the bands corresponding to the C-H bending and C-O stretching were observed on HC-PS-WAS-Scr. In contrast, only the C-O stretching was found on the GAC. These C-O bands may have originated from some methyl ethers, but future studies may be useful to validate this possibility. On the other hand, some important vibrational bands, such as O-H stretching, were not detected on either sample, indicating the tested sample's dryness (absence of water molecules).

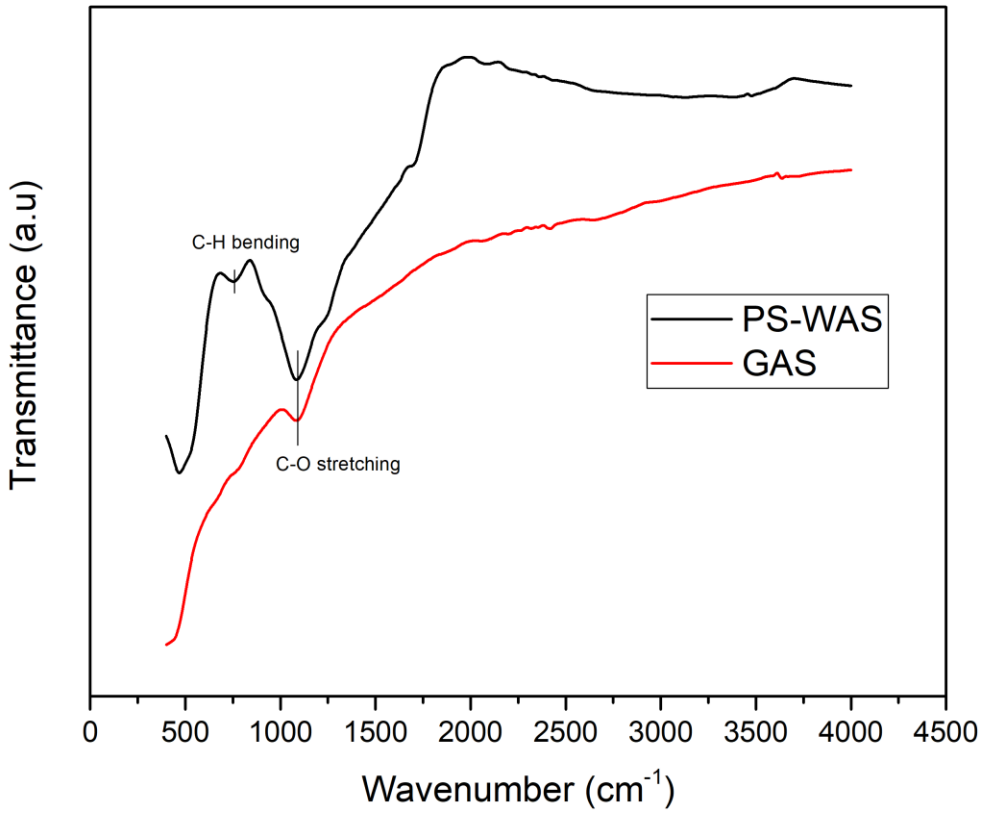

Figure 4-4: FTIR analysis of the tested samples

- *Energy Dispersive Spectroscopy (EDS) mapping*

Each activated carbon sample was marked with five spectra, but only the elemental results of one were shown. **Figure 4.5** displays the predominant elements found in the two activated carbons: carbon and oxygen. The observed GAC in HC-PS-WAS-Scre had a carbon-to-oxygen ratio that was nearly 1:1, with carbon being more abundant. Among the two, GAC had the highest carbon content at 78.8%, while HC-PS-WAS-Scre had a carbon content of 43.4%. While HC-PS-WAS-Scre had a lower carbon content than the other substance, it had a significantly higher oxygen content (40.5%), nearly three times the amount of oxygen found in GAC (13.5%).

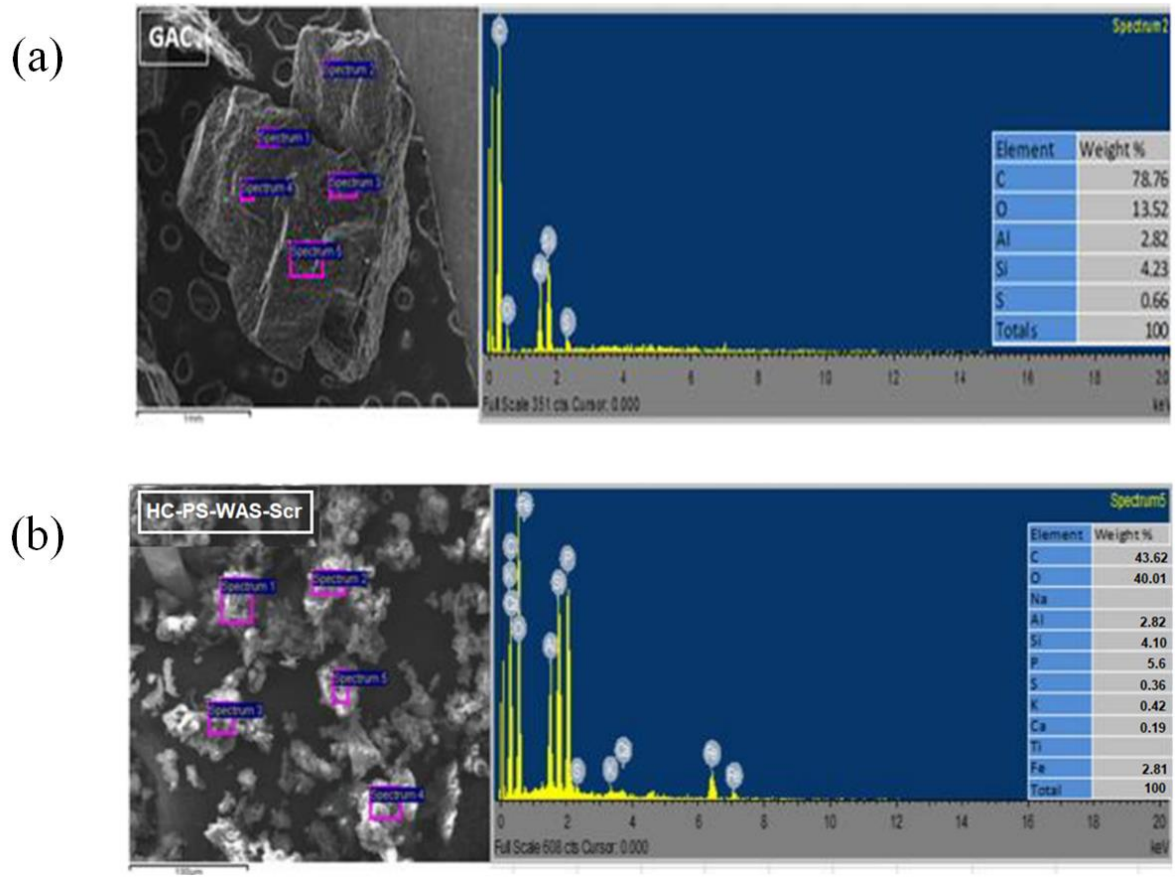

Figure 4-5: EDS spectrum of a) GAC, b) HC-PS-WAS-Scr

4.2 Lead (Pb (II)) adsorption

Lead (Pb (II)) adsorption refers to removing lead ions from a solution by binding them to a solid surface, typically a material with specific adsorption properties. This is a necessary environmental and water treatment process, as lead is a toxic heavy metal that can have detrimental effects on human health and the environment. Various materials can be employed for lead adsorption, and the choice often depends on factors such as cost, availability, and the specific characteristics of the wastewater or solution being treated(Largitte et al., 2016).

4.2.1 Influencing conditions on the adsorption performance

This subsection consists of the evaluation of the potential of the activated carbon prepared under optimal conditions to remove lead (II) ions from simulated wastewater solutions. The effect of contact time, pH, contaminant (Pb2+) concentration, adsorbent dosage, etc., on the adsorption process of the target contaminants is conducted. Finally, well-known models are applied to fit the equilibrium and kinetics data.

4.2.1.1 Effect of solution pH on adsorption of lead (II) ions

In an aqueous solution, the pH value is an essential factor in adsorption processes, as it not only influences the surface charge of the adsorbent but also facilitates the removal of lead by adsorption by affecting the properties of the metal ion(Alabi-Babalola et al., 2023, Onwordi et al., 2019). **Figure 4.6** illustrates the impact of pH on the removal of lead by the three activated carbons. The reduction of lead was least pronounced in the acidic pH range of 2-4,The slight increase in lead removal at pH range of 3-4 can be seen as a balance between the decrease in electrostatic repulsion ,reduction competion from H^+ ions, and potential changes in lead ion speciation and all of which contribute to more effective adsorption . This phenomenon has been extensively debated in the literature and is ascribed to the competition between Pb^{2+} ions and H^+ ions for active sites, which are abundant in acidic environments(Deng et al., 2017, Largitte et al., 2016). The progressive rise in pH resulted in an augmentation in the adsorption of lead due to the presence of negatively charged functional groups on the surface of the adsorbents, rendering them highly accessible for lead adsorption. The optimal pH value for achieving maximum lead removal through true adsorption was determined to be 7 for all two adsorbents. This is because pH values above 7 are thought to promote the formation of lead hydroxide species through precipitation(Alghamdi et al., 2019, Mandal et al., 2023). They found that Lead removal rates above 90% were achieved at a neutral pH. The study emphasized the importance of treating wastewater at a neutral pH because using higher pH values for lead removal would lead to higher post-treatment costs.

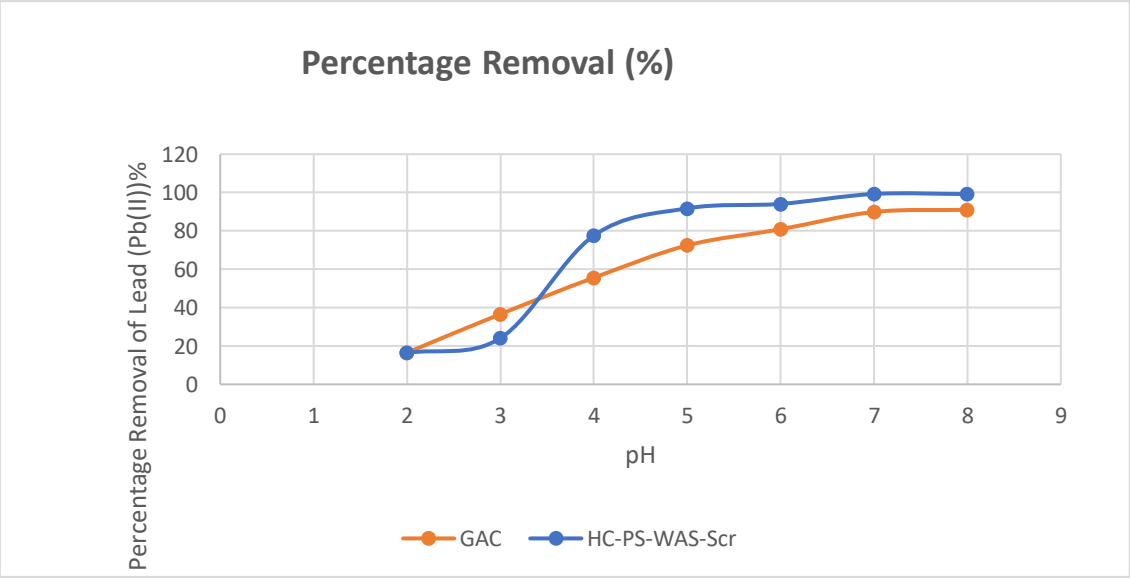

Figure 4-6:Effect of pH on the adsorption of Pb (II) ions - initial concentration: 5.1 mg/L; solution volume: 100 mL, solution pH: 2-8, contact time: 120 min; adsorbent dose: 0.6 g/100 mL).

4.2.1.2 Effect of Dosage on adsorption of lead (II) ions

For the effective uptake of lead ions, it is critical to use the optimal dosage of the adsorbent during the adsorption process; this ensures that the ions have access to active sites(Ranaweera et al., 2020, Ashfaq et al., 2021). The findings presented in **Figure 4.7** indicate that GAC and HC-PS-WAS-Scr exhibited superior lead ion removal efficiency. With an increase in adsorbent dosage from 0.03 g to 0.3 g, the lead ion removal percentage for GAC rose from 97.96 % to 99.96 %, while for HC-PS-WAS-Scr it rose from 92.40% to 94.51%. This indicates that the removal rate exhibited an upward trend in response to the adsorbent dosage. This phenomenon can be explained by the increased surface area or the number of active sites per unit of adsorbate molecules, which enables the Pb (II) ions to more easily adsorb onto the adsorption sites of the activated carbons (Harshananda et al., 2020). After 0.6g, subsequent increases in adsorbent dosage for GAC and HC-PS-WAS-Scr resulted in a constant value, owing to the high capacity for the mole of analyte in the reaction. It generally indicate that the adsorption process has reached equilibrium This means that the maximum adsorption capacity of the adsorbent has been achived and adding more absorbent soes not significant increase the amount of adsorbate being removed from the solution. Furthermore, no substantial enhancements were observed in the Pb (II) ion removal percentage. The phenomenon described may be ascribed to the excessive concentration of adsorbent particles in the solution, which results in the overlap of adsorption sites(Ashfaq et al., 2021).

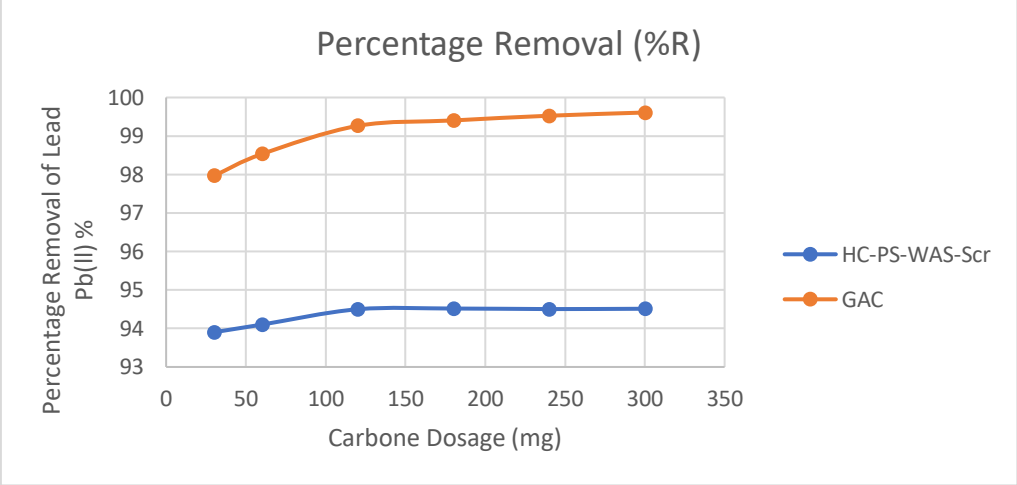

Figure 4-7: Effect of adsorbent dosage on the adsorption of Pb (II) ions - initial concentration: 5.1 mg/L; solution volume: 100 mL, contact time: 120min; adsorbent dose: 0.03-0.3g/100 mL; solution pH: 7

4.2.1.3 Effect of initial concentration on adsorption of lead (II) ions

The initial concentration of the adsorbate is an essential determinant in surmounting any resistance to Pb (II) mass transfer between the aqueous and solid phases(Ranaweera et al., 2020). Furthermore, it

regulates the rate at which the adsorption process occurs, rendering it a critical element that must be considered to achieve effective adsorption. A range of adsorbate concentrations from 2.5 mg/l to 20 mg/l was utilized to examine the impact of concentration on the adsorption process. **Figure 4.8** shows that the percentage of lead ions removed increased initially as the lead ion concentration increased until 5.0 mg/l was reached, across all adsorbents. The percentage of Pb (II) ion removal by HC-PS-WAS-Scre and GAC at a concentration of 5.0 mg/l was 99.996% and 99.98%, respectively. An additional 5 mg/l of concentration resulted in a reduction in the uptake of metal ions by all three adsorbents. The strong interaction between the adsorbate and the numerous active sites of the adsorbent, which are available for adsorption at lower adsorbate concentrations and thus result in greater removal, is responsible for the observed phenomena (Taşar et al., 2014) The saturation of active sites can explain the reduction in removal efficiency at higher concentrations; when the quantity of lead ions increases, the number of active sites on the activated carbon remains constant. Consequently, following the adsorption process, residual ions are in solution (James et al., 2016). The observed reduction in removal efficiency at higher concentrations may also be attributed to the participation of active sites that are energetically unfavourable to adsorption, given that the more favourable sites will be occupied to capacity. Furthermore, elevated ion concentrations give rise to accelerated ion collision and diffusion rates, both of which contribute to a reduction in removal efficiency(Mahmoodi et al., 2011).

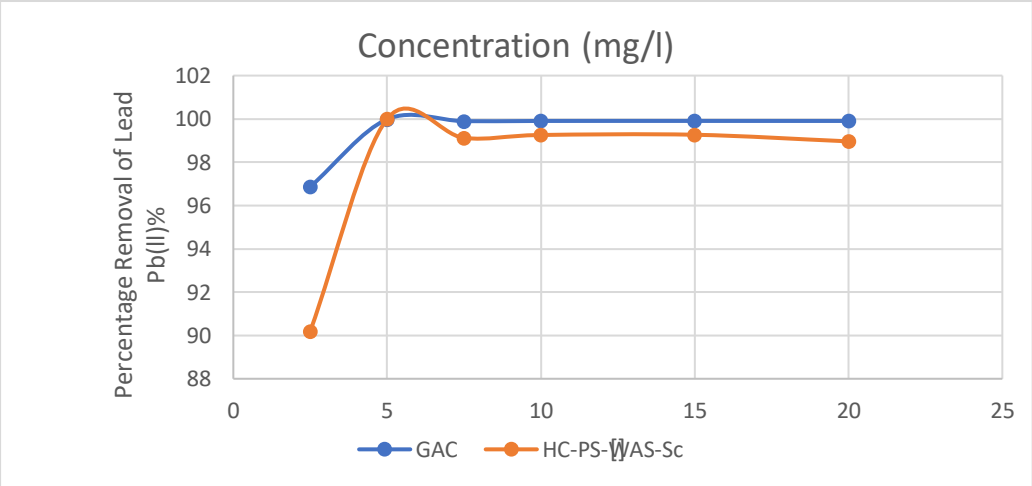

Figure 4-8: Effect of initial concentration on the adsorption of Pb (II) ions - initial concentration: 2.5-20 mg/L; solution volume: 100 mL, contact time: 120 min; adsorbent dose: 0.3 g for GAC and HC-PS-WAS-Scr; solution pH: 7.

4.2.1.4 Effect of contact time on adsorption of lead (II) ions

An experiment was performed to determine the effect of contact time over a range of 10–280 minutes. The optimum conditions, which were determined by varying the parameters in the preceding sections (pH 7, adsorbent dosage of 0.3 g for GAC and HC-PS-WAS-Scr, and initial concentration of 5.0 mg/l), were utilized. **Figure 4.9** below illustrates the correlation between the percentage of lead removal and the contact time. Initially, the adsorption process transpired at a rapid pace. During the initial thirty

minutes, GAC exhibited a removal rate of 97.90%, while HC-PS-WAS-Scr achieved 96.93%. This trend, which indicates a swift decrease in the initial rate of adsorption, might have been facilitated by the activated carbons' exterior surface possessing an adequate quantity of active functional groups and vacant active sites(Ranaweera et al., 2020). Granular activated carbon (GAC) attained equilibrium more rapidly than HC-PS-WAS-Scr; the change in removal percentage was nearly constant from 100 to 280 minutes, with a slight inflection at 160 minutes, indicating that equilibrium had been reached. The HC-PS-WAS-Scr uptake exhibited a marginal decline following 90 minutes, potentially due to active site saturation following the attainment of equilibrium(Asuquo et al., 2017, Mansha et al., 2020). An increase in contact time beyond this threshold has been associated with a decline in removal percentage, as there are fewer available Pb (II) ions to bind to the active sites that remain (Yao et al., 2016). Following this, the rate of uptake exhibited a negligible change. It is worth mentioning that under ideal conditions, HC-PS-WAS-Scr (98.93%) and GAC (99.91%) exhibited the highest percentage removal, respectively.

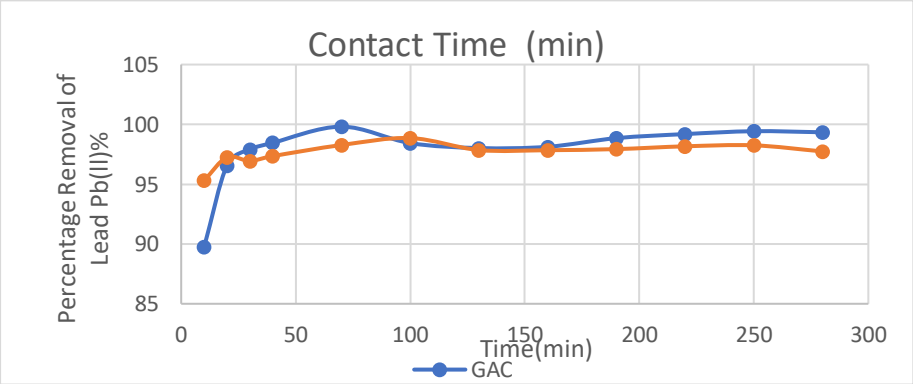

Figure 4-9: Effect of contact time on the adsorption of Pb (II) ions - initial concentration: 5.0 mg/L; solution volume: 100 mL, adsorbent dose: 0.3 g for GAC and HC-PS-WAS-Scr; solution pH: 7.

4.2.2 Isotherm Studies for the Adsorption of Lead (II) Ions

Equilibrium experiments were conducted using optimal adsorbent masses of 0.3g, which had been determined previously. The adsorbent was mixed with 100 ml solution of the appropriate Pb^{2+} solution. The agitation speed of 150 rpm was used for 280 minutes. This experiment was initially done with Pb^{2+} ions, and the concentration range ranged from 2.5 to 20 mg/L. **Figure 4.10** shows the isotherms performed at room temperature on the commercial GAC and the prepared HC-PS-WAS.

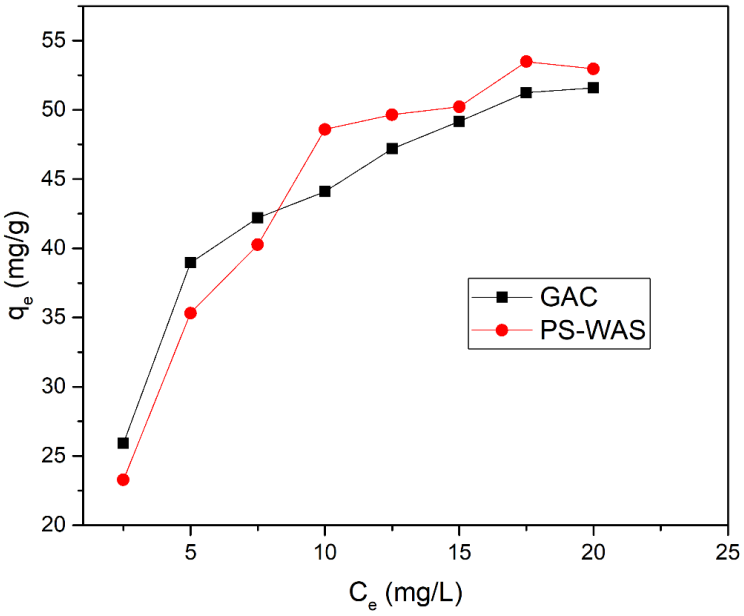

Figure 4-10: Isotherm adsorption of Pb2+ on Commercial granular activated carbon (GAC) and the prepared annealed carbon

These data were fitted with the most linearized isotherm models, namely, Langmuir and Freundlich (Sh. Gohr et al., 2022)as shown in **Figure 4.11**. **Table 4.3** below contains the equations for the Freundlich and Langmuir isotherm models, which were used to examine the experimental results of the two adsorbents. Table 4.3 lists the different parameters of the fit.

Table 4-3: Fitting parameters of the isotherms

Materials	**Langmuir**			**Freundlich**		
	q_e(mg/g)	K_L (L/mg)	R^2	K_F ($mg^{1-1/n}$ $L^{1/n}/g$)	n	R^2
GAC	59.77	0.317	0.998	22.35	3.49	0.916
HC-PS-WAS-Scr	65.61	0.233	0.993	17.69	1.48	0.935

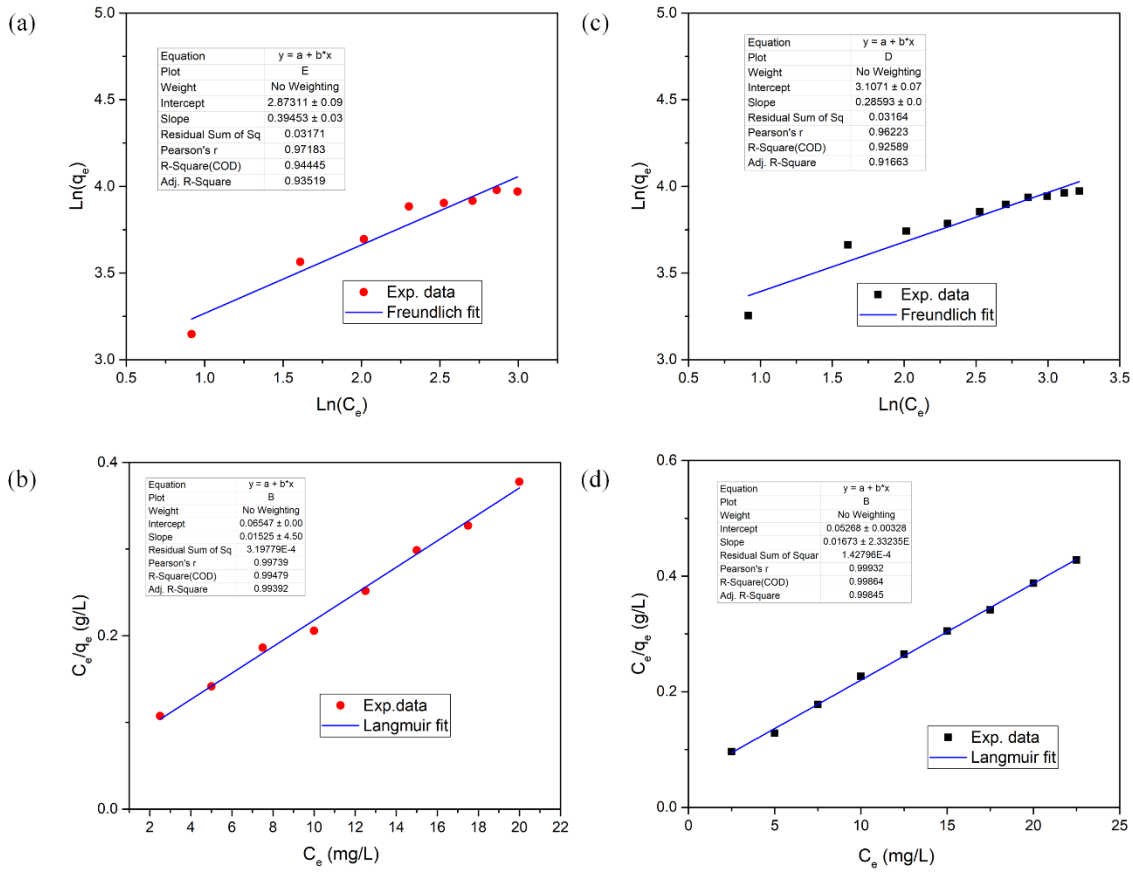

Figure 4-11: Fitting of the isotherm with the Langmuir and Freundlich models; (a), (b)HC-PS-WAS-Scr, (c) and (d) GAC.

The study of the experimental results using the Langmuir and Freundlich isotherms indicates that the data for GAC exhibited a comparable fit for both isotherms (R^2 = 0.998 and 0.916, respectively), with the Langmuir isotherm providing the most accurate fit. The coefficient of determination (R^2) for HC-PS-WAS-Scr was consistently higher for both isotherms, with the R^2 value for the Langmuir isotherm being slightly higher at 0.993(Suresh Jeyakumar and Chandrasekaran, 2014). These findings indicate that the adsorbents GAC and HC-PS-WAS-Scr had multilayers of adsorbate coverage by natural means. The Langmuir equation is typically used when adsorption occurs on uniform surfaces and where the interactions between the adsorbed molecules may be ignored. The Freundlich equation is quite effective in modeling adsorption in aquatic environments. The correlation coefficient exceeds 0.97 for both models, demonstrating a strong agreement between the experimental results and the Langmuir and Freundlich isotherms, as demonstrated in **Figure 4.11**. The isotherm in question does not anticipate any saturation of the sorbent by the sorbate. Consequently, it mathematically predicts an infinite surface coverage, indicating the occurrence of multilayer adsorption on the surface(Ibrahim et al., 2013).

Upon comparing the R^2 values in **Table 4.3**, it is evident that the Freundlich isotherm model outperforms the other isotherm models. The values of K_F and n demonstrate that Pb (II) ions can be easily separated from the aqueous solution, suggesting that adsorption is likely to occur. The K_F value of the intercept

serves as a measure of the adsorbent's adsorption capacity. On the other hand, the slope 1/n reflects the impact of concentration on the adsorption capacity and measures the intensity of adsorption. If n=1, it signifies linear adsorption and uniform adsorption energies across all sites. For values of n greater than 1, it is observed that the marginal adsorption energy increases as the surface concentration increases. **Table 4.3** demonstrates that the n value signifies a strong link between the absorbate and adsorbent, and it also indicates that the surface of the adsorbent is heterogeneous. The Freundlich adsorption capacity of diatomite investigated in this study is consistent with the findings reported by other researchers(Zhang et al., 2013, Salman et al., 2016).

4.2.3 Kinetic studies for Pb (II) ions

Adsorption kinetics examines the rate at which a solute is uptaken, determining how long the adsorbate remains at the solid-solution interface, including the diffusion process. The adsorption mechanism is contingent upon the physical and chemical properties of the adsorbents, as well as the process of mass transfer. The experimental data were utilized to investigate the kinetics of metal ion adsorption.

The kinetics of the two adsorbents were examined at a contact time of 180 minutes and two distinct Pb^{2+} ions concentrations of 10 mg/L and 20 mg/L, and the other experimental conditions were kept fixed. The pseudo-first order, and pseudo-second kinetic models are used to fit the experimental data, and the results are given in Figure 4.12 and 4.13, respectively.

The parameters derived from the plots of the equations are presented in Table 4.4. Upon comparing the characteristics of the two models, it was determined that the Pseudo-second order model was the most appropriate for the kinetic data of both adsorbents, particularly at a concentration of 20mg/L(Suresh Jeyakumar and Chandrasekaran, 2014). The R^2 values for GAC and HC-PS-WAS-Scr at a concentration of 10 mg/L were 0.6484 and 0.907, respectively. The second concentration of 20mg/L resulted in R^2 of 0.9758 and 0.994 for all the adsorbents. The calculated values for GAC and HC-PS-WAS-Scr were 43.38 mg/g and 46.99 mg/g, respectively, at 20 mg/L of Pb^{2+}. As a result, there is a strong correlation between the pseudo-second-order model (PSO) and the adsorption of Pb (II) ions onto the adsorbents (Manjuladevi *et al.*, 2018).

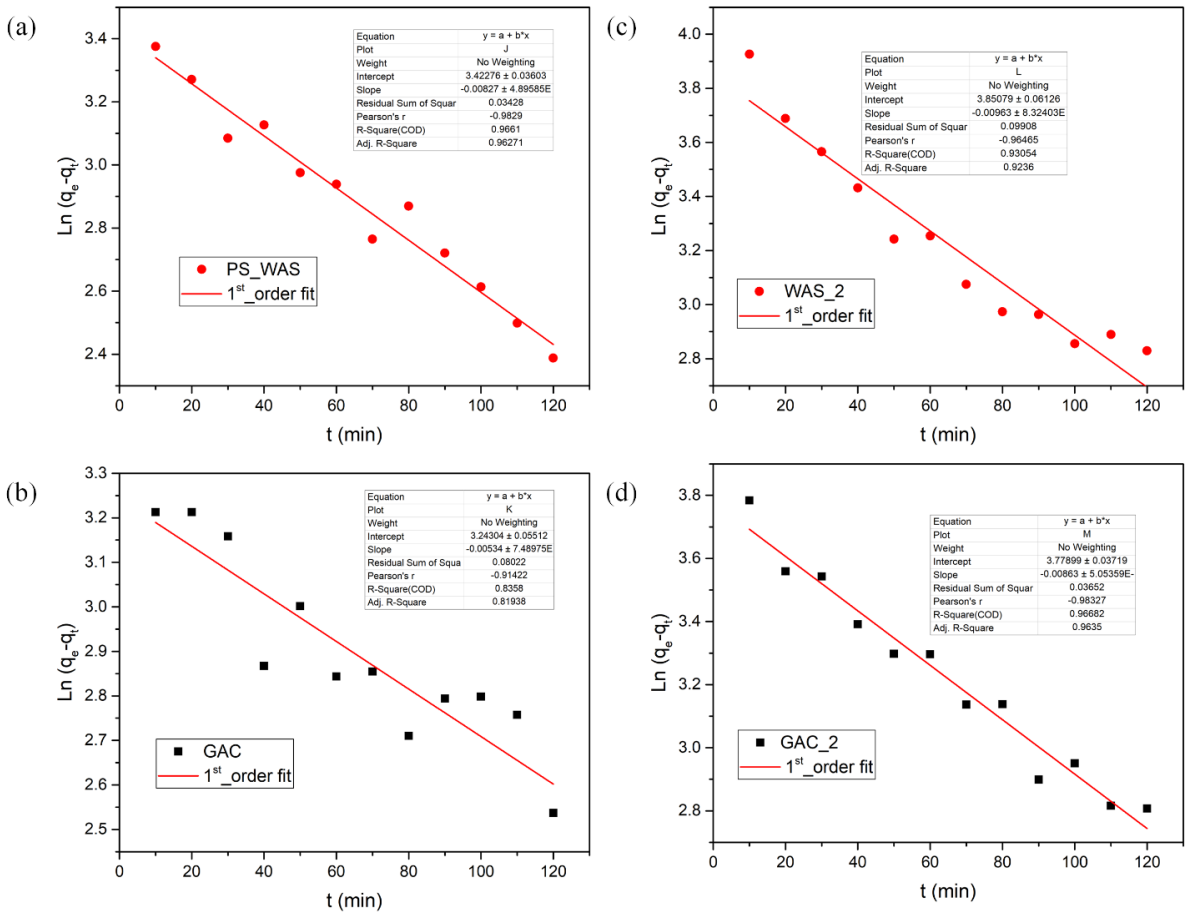

Figure 4-12: Fitting the kinetics with the pseudo-first order kinetic model at different Pb2+ concentrations and adsorbents: at [Pb2+]= 10 mg/L, a)HC-PS-WAS b) GAC; at [Pb2+]= 20 mg/L, c)HC-PS-WAS d) GAC.

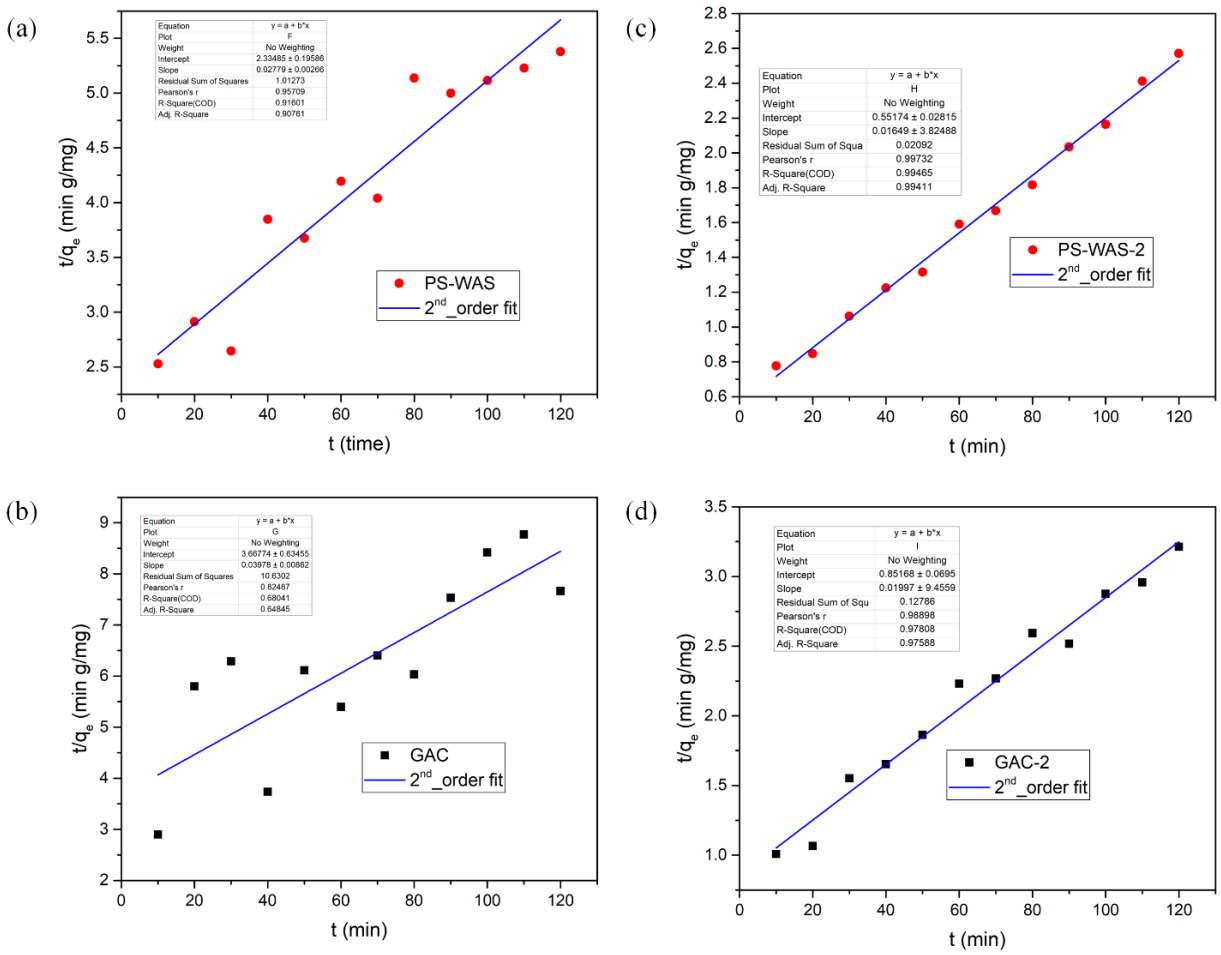

Figure 4-13: Fitting the kinetics with the pseudo-second-order kinetic model at different Pb^{2+} concentrations and adsorbents: at [Pb^{2+}]= 10 mg/L, a)HC-PS-WAS b) GAC; at [Pb^{2+}]= 20 mg/L, c)HC-PS-WAS d) GAC.

Table 4-4:Fitting parameters of the kinetic models at different lead (II) concentrations and adsorbents

[Pb2+] (mg/L)	Materials	Pseudo-first order			Second-order kinetic		
		q_e (mg/g)	K_1 (1/min)	R^2	q_e (mg/L)	K_2 (g/min/mg)	R^2
10	GAC	25.6	0.00053	0.819	25.16	0.108	0.6484
	HC-PS-WAS-Scr	30.6	0.0083	0.962	35.98	0.0119	0.907
20	GAC	43.38	0.0086	0.9635	50.07	0.023	0.9758
	HC-PS-WAS-Scr	46.99	0.0096	0.9236	60.64	0.03	0.994

The properties and adsorption capacity of the prepared activated carbon (HC-PS-WAS-Scr) were ascertained and compared to those of a commercial activated carbon (GAC) according to the objectives set out in Chapter 1 . The findings indicate the successful production of activated carbon from hydrochar and its effectiveness in eliminating lead ions from a water-based solution. Under ideal circumstances, including pH, adsorbent dosage, beginning solute concentration, and equilibrium duration, HC-PS-WAS-Scr outperformed GAC.

5 CONCLUSION

In this chapter, the specific objectives and the concomitant research questions of this study are summarized to present an overview of the study's conclusions and to make a critical evaluation. This study assessed the potential of Hydrochar derived from wastewater sludge (HC-PS-WAS-Scr) as a low-cost adsorbent material for lead (II) removal on synthetic industrial waste metal solutions. To accomplish this overall objective, three research questions were elaborated. The first question regarding the optimal activation conditions for producing hydrochar-based activated carbon with enhanced adsorption properties was answered by conducting intensive experimental works and the main results are summarized as follows:

- HC-PS-WAS-Scr was synthesized by pyrolysis of waste sludge at 450 °C under a nitrogen (N_2) atmosphere. The results from the SEM-EDS micrographs indicated that these samples had a heterogeneous and randomized shape with particle size in the 79-180 μm range and porous structure. The EDS showed that the main elements were carbon (C) and oxygen (O), which translated to a high ash content of about 69.8 % compared to the commercial GAC (2.9 %) with defined clinoptilolite crystals. As a result of this high ash content, its surface area measured by iodine absorption was only 115.21 m^2/g, almost ten times lower than that of GAC (1055 m^2/ g).
- The thermal stability of the HC-PS-WAS-Scr was studied using TGA. The results of the TGA show that the samples continually lost weight after being heated up to 700 °C. This weight loss was not entirely evident, and maybe it could be due to dehydration and dehydroxylation processes. The findings from the FTIR spectra mainly showed the presence of a peak corresponding to C-O stretching and the absence of other functional groups, such as carboxyl and hydroxyl. This was due to the physical activation route conducted in this study.
- The effects of process parameters such as pH, adsorbent dosage, contact time, and initial metal ion concentration on Pb^{2+} removal efficiencies were investigated in detail. The equilibrium studies showed that HC-PS-WAS can be used as an excellent adsorbent for removing heavy metals from synthetic wastewater solutions. The results showed that the maximum lead (II) removal capacities Q_m of HC-PS-WAS and GAC were 66 and ~ 60 mg/g, respectively. Moreover, the results indicated that the removal capacity increased with the initial solution pH, i.e., the removal efficiency rapidly increased from 20 to 100 % with the pH increment from 2 to 7.
- The Langmuir and Freundlich isotherm models were tested to characterize the experimental data and assess the adsorption behavior of HC-PS-WAS and GAC for lead. It was noted that the experimental data was better fitted to the Langmuir isotherm than the Freundlinch

isotherm. The value of the correlation coefficients R^2 ranged from 0.993 to 0.998 for the Langmuir isotherm and from 0.916 to 0.935 for the Freundlich isotherm.

- The effects of initial solution concentration and contact time on the Pb^{2+} removal efficiency of GAC and HC-PS-WAS were analyzed. The results showed that the optimum contact time was above 90 minutes. The results from the kinetic study indicated that the Pb^{2+} removal capacity increased with an initial high Pb^{2+} solution concentration of 20 mg/L compared to that of 10 mg/L. Additionally, the results indicated that the adsorption Pb^{2+} on the selected adsorbents involves a complex mechanism and several possible rate-controlling steps, including pseudo-first and second-order reaction kinetics. However, it was noted that the kinetic data fits the pseudo-second-order reaction better than the pseudo-first order at a higher initial lead(II) concentration. The value of the correlation coefficients R^2 ranged from 0.975 to 0.994 for the second-order and from 0.923 to 0.963 for the Freundlich isotherm.

From these two latter point the second research question was answered. It can be seen that, Langmuir isotherms and pseudo-second order kinetics models well described the removal efficiency of the target micropollutants using the hydrochar-based activated carbon. Moreover, the initial stated hypothesis turned out to be valid, which is HC-PS-WAS has a better lead (II) removal efficiency than GAC.

Recommended Future Work

The experiments presented in this thesis have shown that both HC-PS-WAS can be used in treating wastewater. Although the initial goals were achieved in this study, some other aspects were not within the scope of this study due to the time limitations and availability of Lab equipment. Therefore, further research and studies are needed, taking into account in order to ascertain the efficacy of low-cost HC-PS-WAS in heavy metals removal. There are several areas of research that still require exploration in order to give better perspectives in terms of possible applications. Some recommendations for further studies are presented below:

- Although the effects of the adsorbent mass, initial solution pH, initial solution concentration, contact time, agitation speed, and the type of the adsorbent were systematically studied, the effect of temperature on heavy metal and particularly Pb^{2+} removal capacity was not included. This aspect (temperature variation) could give some valuable insights in applied purposes on a large scale where wastewater in changing climate conditions (winter, summer) should be processed. Therefore, studies involving the simultaneous impact of all these factors are welcomed.
- Kinetic and equilibrium studies were performed throughout this study with solutions only containing Pb^{2+} cations, while in practice, wastewater contains a combination of cations such as Cu^{2+}, Fe^{2+}, Zn^{2+}, and so on. Therefore, as a further study, adsorption studies of a mixture of heavy metals in solution should be undertaken to ascertain each heavy metal's selectivity.

References

ACHARYA, J., SAHU, J., MOHANTY, C. & MEIKAP, B. 2009. Removal of lead (II) from wastewater by activated carbon developed from Tamarind wood by zinc chloride activation. *Chemical engineering journal,* 149**,** 249-262.

AHMARUZZAMAN, M. 2010. A review on the utilization of fly ash. *Progress in energy and combustion science,* 36**,** 327-363.

AHMED, M. J. & THEYDAN, S. K. 2012. Physical and chemical characteristics of activated carbon prepared by pyrolysis of chemically treated date stones and its ability to adsorb organics. *Powder Technology,* 229**,** 237-245.

ALABI-BABALOLA, O., ARANSIOLA, E., ASUQUO, E., GARFORTH, A. & D'AGOSTINO, C. 2023. Production of Highly Efficient Activated Carbons for Wastewater Treatment from Post-Consumer PET Plastic Bottle Waste. *ChemPlusChem***,** e202300484.

ALCAÑIZ-MONGE, J., ROMÁN-MARTÍNEZ, M. D. C. & LILLO-RÓDENAS, M. Á. 2022. Chemical activation of lignocellulosic precursors and residues: what else to consider? *Molecules,* 27**,** 1630.

ALGHAMDI, A. A., AL-ODAYNI, A.-B., SAEED, W. S., AL-KAHTANI, A., ALHARTHI, F. A. & AOUAK, T. 2019. Efficient adsorption of lead (II) from aqueous phase solutions using polypyrrole-based activated carbon. *Materials,* 12**,** 2020.

ALMAHBASHI, N., KUTTY, S., AYOUB, M., NOOR, A., SALIHI, I., AL-NINI, A., JAGABA, A., ALDHAWI, B. & GHALEB, A. 2021. Optimization of preparation conditions of sewage sludge based activated carbon. *Ain Shams Engineering Journal,* 12**,** 1175-1182.

ANIRUDHAN, T. & SREEKUMARI, S. 2011. Adsorptive removal of heavy metal ions from industrial effluents using activated carbon derived from waste coconut buttons. *Journal of Environmental Sciences,* 23**,** 1989-1998.

ASHFAQ, A., NADEEM, R., BIBI, S., RASHID, U., HANIF, M. A., JAHAN, N., ASHFAQ, Z., AHMED, Z., ADIL, M. & NAZ, M. 2021. Efficient adsorption of lead ions from synthetic wastewater using agrowaste-based mixed biomass (potato peels and banana peels). *Water,* 13**,** 3344.

ASUQUO, E., MARTIN, A., NZEREM, P., SIPERSTEIN, F. & FAN, X. 2017. Adsorption of Cd(II) and Pb(II) ions from aqueous solutions using mesoporous activated carbon adsorbent: Equilibrium, kinetics and characterisation studies. *Journal of Environmental Chemical Engineering,* 5**,** 679-698.

BARESEL, C., HARDING, M. & FANG, J. 2019. Ultrafiltration/granulated active carbon-biofilter: efficient removal of a broad range of micropollutants. *Applied Sciences,* 9**,** 710.

BECKER, D. C., BECKER, R. J., CONLEY, W. R., GARNELL, M. A., GRIMES, B., HARRIS, R. H., HARRIS, W. L., HOLDREN, F. J., INHOFFER, W. R. & POPALISKY, J. R. 1974. AWWA Standard for Granular Activated Carbon. *J. Am. Water Work Assoc.,* 66**,** 672-681.

BELOUSOV, A. S., SULEIMANOV, E. V. & PARKHACHEVA, A. A. 2022. Visible light-induced degradation of organic dyes by niobium tellurium oxides ANbTeO6 (A = Rb, Cs) with β-pyrochlore structure. *Materials Letters,* 327**,** 133081.

BHATNAGAR, A., HOGLAND, W., MARQUES, M. & SILLANPÄÄ, M. 2013. An overview of the modification methods of activated carbon for its water treatment applications. *Chemical Engineering Journal,* 219**,** 499-511.

BOUCHELTA, C., MEDJRAM, M. S., BERTRAND, O. & BELLAT, J.-P. 2008. Preparation and characterization of activated carbon from date stones by physical activation with steam. *Journal of Analytical and Applied Pyrolysis,* 82**,** 70-77.

BRETON, R. & BOXALL, A. 2003. Pharmaceuticals and personal care products in the environment: regulatory drivers and research needs. *QSAR & Combinatorial Science,* 22**,** 399-409.

BRUNAUER, S., EMMETT, P. H. & TELLER, E. 1938. Adsorption of Gases in Multimolecular Layers. *Journal of the American Chemical Society,* 60**,** 309-319.

BYAMBA-OCHIR, N., SHIM, W. G., BALATHANIGAIMANI, M. S. & MOON, H. 2016. Highly porous activated carbons prepared from carbon rich Mongolian anthracite by direct NaOH activation. *Applied Surface Science,* 379**,** 331-337.

CAMPOS, N. F., BARBOSA, C. M. B. M., RODRÍGUEZ-DÍAZ, J. M. & DUARTE, M. M. M. B. 2018. Removal of naphthenic acids using activated charcoal: Kinetic and equilibrium studies. *Adsorption Science & Technology,* 36**,** 1405-1421.

CERÓN-RIVERA, M., DÁVILA-JIMÉNEZ, M. M. & ELIZALDE-GONZÁLEZ, M. P. 2004. Degradation of the textile dyes Basic yellow 28 and Reactive black 5 using diamond and metal alloys electrodes. *Chemosphere,* 55**,** 1-10.

CHAKRABORTY, S., CHAKRABORTY, N., MONDAL, S. & PAL, M. 2022. Band gap engineered Sn-doped bismuth ferrite nanoparticles for visible light induced ultrafast methyl blue degradation. *Ceramics International,* 48**,** 37253-37263.

CHENG, D., NGO, H. H., GUO, W., CHANG, S. W., NGUYEN, D. D., LIU, Y., WEI, Q. & WEI, D. 2020. A critical review on antibiotics and hormones in swine wastewater: Water pollution problems and control approaches. *Journal of Hazardous Materials,* 387**,** 121682.

CHEOK, Q. H. N. 2013. *Activated Carbon Manufacture: An opportunity for sustainable management of problematic waste biomass.* Imperial College London.

CHIA, C. H., GONG, B., JOSEPH, S. D., MARJO, C. E., MUNROE, P. & RICH, A. M. 2012. Imaging of mineral-enriched biochar by FTIR, Raman and SEM–EDX. *Vibrational Spectroscopy,* 62**,** 248-257.

CRINI, G., TORRI, G., LICHTFOUSE, E., KYZAS, G. Z., WILSON, L. D. & MORIN-CRINI, N. 2019. Dye removal by biosorption using cross-linked chitosan-based hydrogels. *Environmental Chemistry Letters,* 17**,** 1645-1666.

D4607-94, A. 2006. Standard Test Method for Determination of Iodine Number of Activated Carbon. *In:* MATERIALS, A. S. F. T. A. (ed.).

DE CAPRARIIS, B., DE FILIPPIS, P., HERNANDEZ, A. D., PETRUCCI, E., PETRULLO, A., SCARSELLA, M. & TURCHI, M. 2017. Pyrolysis wastewater treatment by adsorption on biochars produced by poplar biomass. *Journal of environmental management,* 197**,** 231-238.

DE FILIPPIS, P., DI PALMA, L., PETRUCCI, E., SCARSELLA, M. & VERDONE, N. 2013. Production and characterization of adsorbent materials from sewage sludge by pyrolysis. *Chemical Engineering Transactions*.

DENG, J., LIU, Y., LIU, S., ZENG, G., TAN, X., HUANG, B., TANG, X., WANG, S., HUA, Q. & YAN, Z. 2017. Competitive adsorption of Pb (II), Cd (II) and Cu (II) onto chitosan-pyromellitic dianhydride modified biochar. *Journal of colloid and interface science,* 506**,** 355-364.

DOYLE, J., JOHNSON, B. & DOSTIE, P. 2018. Eelgrass Bed Carbon Storage in Casco Bay.

EVBUOMWAN, B., AGBEDE, A. & ATUKA, M. 2013. A comparative study of the physico-chemical properties of activated carbon from oil palm waste (kernel shell and fibre). *International Journal of Science and Engineering Investigations,* 2**,** 75-79.

EVERSON, R. C., NEOMAGUS, H. W., KAITANO, R., FALCON, R., VAN ALPHEN, C. & DU CANN, V. M. 2008. Properties of high ash char particles derived from inertinite-rich coal: 1. Chemical, structural and petrographic characteristics. *Fuel,* 87**,** 3082-3090.

FACCHIN, A., KÜÇÜKAĞA, Y., FABBRI, D. & TORRI, C. 2023. Analytical evaluation of the coupling of hydrothermal carbonization and pyrolysis (HTC-Py) for the obtainment of bioavailable products. *Journal of Analytical and Applied Pyrolysis,* 175**,** 106185.

FAN, L., ZHOU, Y., YANG, W., CHEN, G. & YANG, F. 2008. Electrochemical degradation of aqueous solution of Amaranth azo dye on ACF under potentiostatic model. *Dyes and Pigments,* 76**,** 440-446.

FAROOQ, S., CAI, R., MCGETTRICK, J., PEAN, E., DAVIES, M., AL HARRASI, A. S., PALMER, R. & TIZAOUI, C. 2023. Visible-light induced photocatalytic degradation of estrone (E1) with hexagonal copper selenide nanoflakes in water. *Process Safety and Environmental Protection,* 172**,** 1-15.

FU, D., KURNIAWAN, T. A., GUI, H., LI, H., FENG, S., LI, Q. & WANG, Y. 2022. Role of CuxO-Anchored Pyrolyzed Hydrochars on H2O2-Activated Degradation of Tetracycline: Effects of Pyrolysis Temperature and pH. *Industrial & Engineering Chemistry Research,* 61**,** 8847-8857.

GARCIA, X. & PARGAMENT, D. 2015. Reusing wastewater to cope with water scarcity: Economic, social and environmental considerations for decision-making. *Resources, Conservation and Recycling,* 101**,** 154-166.

GHOSH, A., DA SILVA SANTOS, A. M., CUNHA, J. R., DASGUPTA, A., FUJISAWA, K., FERREIRA, O. P., LOBO, A. O., TERRONES, M., TERRONES, H. & VIANA, B. C. 2018. CO2 Sensing by in-situ Raman spectroscopy using activated carbon generated from mesocarp of babassu coconut. *Vibrational Spectroscopy,* 98**,** 111-118.

GILES, C. H., SMITH, D. & HUITSON, A. 1974. A general treatment and classification of the solute adsorption isotherm. I. Theoretical. *Journal of Colloid and Interface Science,* 47**,** 755-765.

GRATUITO, M. K. B., PANYATHANMAPORN, T., CHUMNANKLANG, R. A., SIRINUNTAWITTAYA, N. & DUTTA, A. 2008. Production of activated carbon from coconut shell: Optimization using response surface methodology. *Bioresource Technology,* 99**,** 4887-4895.

GRAVEL, G. 2020. Gimme a Break: The Patent Term Restoration Act Should Give Environmental Innovators a Chance to Catch a (Cleaner) Breath. *J. Intell. Prop. L.,* 28**,** 413.

GROVER, V. I. 2006. *Water: Global Common and Global Problems*, Taylor & Francis.

GUO, S., GAO, Y., WANG, Y., LIU, Z., WEI, X., PENG, P., XIAO, B. & YANG, Y. 2019. Urea/ZnCl(2) in situ hydrothermal carbonization of Camellia sinensis waste to prepare N-doped biochar for heavy metal removal. *Environ Sci Pollut Res Int,* 26**,** 30365-30373.

GUTIÉRREZ, M., GRILLINI, V., MUTAVDŽIĆ PAVLOVIĆ, D. & VERLICCHI, P. 2021. Activated carbon coupled with advanced biological wastewater treatment: A review of the enhancement in micropollutant removal. *Science of The Total Environment,* 790**,** 148050.

HAIMOUR, N. M. & EMEISH, S. 2006. Utilization of date stones for production of activated carbon using phosphoric acid. *Waste Management,* 26**,** 651-660.

HARSHANANDA, T., AYISHA, T., JANANI PRIYANKA, P., KN, D. M. & VIJAYAKUMAR, R. 2020. Removal of colour from textile effluent by adsorption using banana stem and coffee husk: a review. *J Mech Civ Eng,* 17**,** 32-41.

HELCOM, O. 2003. Declaration of the first Joint Ministerial Meeting of the Helsinki and OSPAR Commissions. Bremen.

HINA, H., NAFEES, M. & AHMAD, T. 2021. Treatment of industrial wastewater with gamma irradiation for removal of organic load in terms of biological and chemical oxygen demand. *Heliyon,* 7**,** e05972.

HO, Y. S. & MCKAY, G. 1999a. A kinetic study of dye sorption by biosorbent waste product pith. *Resources, Conservation and Recycling,* 25**,** 171-193.

HO, Y. S. & MCKAY, G. 1999b. Pseudo-second order model for sorption processes. *Process Biochemistry,* 34**,** 451-465.

HUANG, F.-C., LEE, C.-K., HAN, Y.-L., CHAO, W.-C. & CHAO, H.-P. 2014. Preparation of activated carbon using micro-nano carbon spheres through chemical activation. *Journal of the Taiwan Institute of Chemical Engineers,* 45**,** 2805-2812.

HUNGER, K. 2003. *Industrial dyes : chemistry, properties, application,* Weinheim, Wiley-VCH Weinheim.

IBRAHIM, H. S., EL-KADY, A. A., AMMAR, N. S., MEESUK, L., WATHANAKUL, P. & ABDEL-WAHHAB, M. A. 2013. Application of isotherm and kinetic models for the removal of lead ions from aqueous solutions. *Journal of Environmental Engineering,* 139**,** 349-357.

IGHALO, J. O., RANGABHASHIYAM, S., DULTA, K., UMEH, C. T., IWUOZOR, K. O., ANIAGOR, C. O., ESHIEMOGIE, S. O., IWUCHUKWU, F. U. & IGWEGBE, C. A. 2022. Recent advances in hydrochar application for the adsorptive removal of wastewater pollutants. *Chemical Engineering Research and Design,* 184**,** 419-456.

IOANNIDOU, O. & ZABANIOTOU, A. 2007. Agricultural residues as precursors for activated carbon production—A review. *Renewable and Sustainable Energy Reviews,* 11**,** 1966-2005.

JAMES, D., SURENDRAN, S., IFELEBUEGU, A., GANJIAN, E. & KINUTHIA, J. Grey water reclamation for urban non-potable reuse–challenges and solutions: a review. 7th International Conference on Sustainable Built Environment 2016 Kandy, Sri Lanka.

JANSEN, R. J. J. & VAN BEKKUM, H. 1994. Amination and ammoxidation of activated carbons. *Carbon,* 32**,** 1507-1516.

JEFFERSON, B., LAINE, A., PARSONS, S., STEPHENSON, T. & JUDD, S. 2000. Technologies for domestic wastewater recycling. *Urban Water,* 1**,** 285-292.

JINDO, K., MIZUMOTO, H., SAWADA, Y., SANCHEZ-MONEDERO, M. A. & SONOKI, T. 2014. Physical and chemical characterization of biochars derived from different agricultural residues. *Biogeosciences,* 11**,** 6613-6621.

JJAGWE, J., OLUPOT, P. W., MENYA, E. & KALIBBALA, H. M. 2021. Synthesis and application of Granular activated carbon from biomass waste materials for water treatment: A review. *Journal of Bioresources and Bioproducts,* 6**,** 292-322.

KALE, A. Study on attrition of carbon particles during regeneration of activated carbon. World Gold, 2019.

KATZ, S., PEVZNER, A., SHEPELEV, V., MARX, S., ROTTER, H., AMITAY-ROSEN, T. & NIR, I. 2022. Activated carbon aging processes characterization by Raman spectroscopy. *MRS Advances***,** 1-4.

KENNEDY, A. M. & SUMMERS, R. S. 2015. Effect of DOM size on organic micropollutant adsorption by GAC. *Environmental science & technology,* 49**,** 6617-6624.

KOPRIVICA, M., SIMIĆ, M., PETROVIĆ, J., ERCEGOVIĆ, M. & DIMITRIJEVIĆ, J. 2023. Evaluation of Adsorption Efficiency on Pb(II) Ions Removal Using Alkali-Modified Hydrochar from Paulownia Leaves. *Processes* [Online], 11.

KÖSEOĞLU, E. & AKMIL-BAŞAR, C. 2015. Preparation, structural evaluation and adsorptive properties of activated carbon from agricultural waste biomass. *Advanced Powder Technology,* 26**,** 811-818.

KOSHELEVA, R. I., MITROPOULOS, A. C. & KYZAS, G. Z. 2019. Synthesis of activated carbon from food waste. *Environmental Chemistry Letters,* 17**,** 429-438.

LANGMUIR, I. 1918. THE ADSORPTION OF GASES ON PLANE SURFACES OF GLASS, MICA AND PLATINUM. *Journal of the American Chemical Society,* 40**,** 1361-1403.

LARGITTE, L., BRUDEY, T., TANT, T., DUMESNIL, P. C. & LODEWYCKX, P. 2016. Comparison of the adsorption of lead by activated carbons from three lignocellulosic precursors. *Microporous and Mesoporous Materials,* 219**,** 265-275.

LEE, K. E., MORAD, N., TENG, T. T. & POH, B. T. 2012. Development, characterization and the application of hybrid materials in coagulation/flocculation of wastewater: A review. *Chemical Engineering Journal,* 203**,** 370-386.

LEFEBVRE, O. & MOLETTA, R. 2006. Treatment of organic pollution in industrial saline wastewater: A literature review. *Water Research,* 40**,** 3671-3682.

LIANG, Y., ZHU, Y., LIU, C., LEE, K.-R., HUNG, W.-S., WANG, Z., LI, Y., ELIMELECH, M., JIN, J. & LIN, S. 2020. Polyamide nanofiltration membrane with highly uniform sub-nanometre pores for sub-1 Å precision separation. *Nature communications,* 11**,** 1-9.

LIM, S., SHI, J. L., VON GUNTEN, U. & MCCURRY, D. L. 2022. Ozonation of organic compounds in water and wastewater: A critical review. *Water Research,* 213**,** 118053.

LING, Y., WANG, H., FEI, X., HUANG, T., SHAN, Q., HEI, D., CHEN, T., ZHANG, X. & JIA, W. 2022. Enhancement effect of γ-irradiation pre-treatment on anaerobic digestion performance of kitchen wastewater. *Journal of Cleaner Production,* 330**,** 129951.

LUO, X., HUANG, Z., LIN, J., LI, X., QIU, J., LIU, J. & MAO, X. 2020. Hydrothermal carbonization of sewage sludge and in-situ preparation of hydrochar/MgAl-layered double hydroxides composites for adsorption of Pb(II). *Journal of Cleaner Production,* 258**,** 120991.

MA, Y., HU, J. & YE, G. 2013. The pore structure and permeability of alkali activated fly ash. *Fuel,* 104**,** 771-780.

MAHMOODI, N. M., NAJAFI, F., KHORRAMFAR, S., AMINI, F. & ARAMI, M. 2011. Synthesis, characterization and dye removal ability of high capacity polymeric adsorbent: Polyaminoimide homopolymer. *Journal of Hazardous Materials,* 198**,** 87-94.

MANCHISI, J., MATINDE, E., ROWSON, N. A., SIMMONS, M. J. H., SIMATE, G. S., NDLOVU, S. & MWEWA, B. 2020. Ironmaking and Steelmaking Slags as Sustainable Adsorbents for Industrial Effluents and Wastewater Treatment: A Critical Review of Properties, Performance, Challenges and Opportunities. *Sustainability,* 12**,** 2118.

MANDAL, S., HWANG, S., MARPU, S. B., OMARY, M. A., PRYBUTOK, V. & SHI, S. Q. 2023. Bioinspired synthesis of silver nanoparticles for the remediation of toxic pollutants and enhanced antibacterial activity. *Biomolecules,* 13**,** 1054.

MANJULADEVI, M., ANITHA, R. & MANONMANI, S. 2018. Kinetic study on adsorption of Cr (VI), Ni (II), Cd (II) and Pb (II) ions from aqueous solutions using activated carbon prepared from Cucumis melo peel. *Applied water science,* 8**,** 1-8.

MANSHA, M., WAHEED, A., AHMAD, T., KAZI, I. W. & ULLAH, N. 2020. Synthesis of a novel polysuccinimide based resin for the ultrahigh removal of anionic azo dyes from aqueous solution. *Environmental Research,* 184**,** 109337.

MANSOUR, F., AL-HINDI, M., YAHFOUFI, R., AYOUB, G. M. & AHMAD, M. N. 2018. The use of activated carbon for the removal of pharmaceuticals from aqueous solutions: a review. *Reviews in Environmental Science and Bio/Technology,* 17**,** 109-145.

MARIANA, M., H.P.S, A. K., MISTAR, E. M., YAHYA, E. B., ALFATAH, T., DANISH, M. & AMAYREH, M. 2021. Recent advances in activated carbon modification techniques for enhanced heavy metal adsorption. *Journal of Water Process Engineering,* 43**,** 102221.

MEDHAT, A., EL-MAGHRABI, H. H., ABDELGHANY, A., MENEM, N. M. A., RAYNAUD, P., MOUSTAFA, Y. M., ELSAYED, M. A. & NADA, A. A. 2021. Efficiently activated carbons from corn cob for methylene blue adsorption. *Applied Surface Science Advances,* 3**,** 100037.

MISRAN, E., BANI, O., SITUMEANG, E. M. & PURBA, A. S. 2022. Banana stem based activated carbon as a low-cost adsorbent for methylene blue removal: Isotherm, kinetics, and reusability. *Alexandria Engineering Journal,* 61**,** 1946-1955.

MKUNGUNUGWA, T., MANHOKWE, S., CHAWAFAMBIRA, A. & SHUMBA, M. 2021. Synthesis and characterisation of activated carbon obtained from Marula (Sclerocarya birrea) nutshell. *Journal of Chemistry,* 2021**,** 1-9.

MOLINA-SABIO, M. & RODRíGUEZ-REINOSO, F. 2004. Role of chemical activation in the development of carbon porosity. *Colloids and Surfaces A: Physicochemical and Engineering Aspects,* 241**,** 15-25.

MOUSSA, D. T., EL-NAAS, M. H., NASSER, M. & AL-MARRI, M. J. 2017. A comprehensive review of electrocoagulation for water treatment: Potentials and challenges. *Journal of Environmental Management,* 186**,** 24-41.

MUDHOO, A., CHU, K. H. & MONDAL, P. 2023. Attrition resistance, a sporadically studied factor in aqueous adsorption: Status quo and research outlook towards creating better adsorbents. *Particuology,* 77**,** 71-78.

NASIRUDDIN KHAN, M. & SARWAR, A. 2007. DETERMINATION OF POINTS OF ZERO CHARGE OF NATURAL AND TREATED ADSORBENTS. *Surface Review and Letters,* 14**,** 461-469.

NAUMCZYK, J., SZPYRKOWICZ, L. & ZILIO-GRANDI, F. 1996. Electrochemical treatment of textile wastewater. *Water Science and Technology,* 34**,** 17-24.

NJOKU, V. O., FOO, K. Y., ASIF, M. & HAMEED, B. H. 2014. Preparation of activated carbons from rambutan (Nephelium lappaceum) peel by microwave-induced KOH activation for acid yellow 17 dye adsorption. *Chemical Engineering Journal,* 250**,** 198-204.

NZEDIEGWU, C., NAETH, M. A. & CHANG, S. X. 2021. Lead(II) adsorption on microwave-pyrolyzed biochars and hydrochars depends on feedstock type and production temperature. *Journal of Hazardous Materials,* 412**,** 125255.

ONWORDI, C. T., UCHE, C. C., AMEH, A. E. & PETRIK, L. F. 2019. Comparative study of the adsorption capacity of lead (II) ions onto bean husk and fish scale from aqueous solution. *Journal of water reuse and desalination,* 9**,** 249-262.

ORLANDO, A., FRANCESCHINI, F., MUSCAS, C., PIDKOVA, S., BARTOLI, M., ROVERE, M. & TAGLIAFERRO, A. 2021. A comprehensive review on Raman spectroscopy applications. *Chemosensors,* 9**,** 262.

PALLARÉS, J., GONZÁLEZ-CENCERRADO, A. & ARAUZO, I. 2018. Production and characterization of activated carbon from barley straw by physical activation with carbon dioxide and steam. *Biomass and Bioenergy,* 115**,** 64-73.

PASTUSZAK, M., BRYHN, A. C., HÅKANSON, L., STÅLNACKE, P., ZALEWSKI, M. & WODZINOWSKI, T. 2018. Reduction of nutrient emission from Polish territory into the Baltic Sea (1988–2014) confronted with real environmental needs and international requirements. *Oceanological and Hydrobiological Studies,* 47**,** 140-166.

PRAMODBABU, R., RAI, S., PANDIT, S., PATIL, P., BANERJEE, S., MATHURIYA, A. S. & PRASAD, R. 2021. Chapter 9 - Anaerobic membrane bioreactor for waste water treatment: present state of the art. *In:* SHAH, M. P. & RODRIGUEZ-COUTO, S. (eds.) *Membrane-Based Hybrid Processes for Wastewater Treatment.* Elsevier.

QASEM, N. A. A., MOHAMMED, R. H. & LAWAL, D. U. 2021. Removal of heavy metal ions from wastewater: a comprehensive and critical review. *npj Clean Water,* 4**,** 36.

RAMBABU, N., RAO, B. V. S. K., SURISETTY, V. R., DAS, U. & DALAI, A. K. 2015. Production, characterization, and evaluation of activated carbons from de-oiled canola meal for environmental applications. *Industrial Crops and Products,* 65**,** 572-581.

RANAWEERA, K. H., GODAKUMBURA, P. I. & PERERA, B. A. 2020. Adsorptive removal of Co (II) in aqueous solutions using clearing nut seed powder. *Heliyon,* 6.

RIVERA-UTRILLA, J., SÁNCHEZ-POLO, M., GÓMEZ-SERRANO, V., ÁLVAREZ, P., ALVIM-FERRAZ, M. & DIAS, J. 2011. Activated carbon modifications to enhance its water treatment applications. An overview. *Journal of hazardous materials,* 187**,** 1-23.

ROGOWSKA, J., CIESZYNSKA-SEMENOWICZ, M., RATAJCZYK, W. & WOLSKA, L. 2020. Micropollutants in treated wastewater. *Ambio,* 49**,** 487-503.

SALMAN, T., TEMEL, F., TURAN, N. & ARDALı, Y. 2016. Adsorption of lead (II) ions onto diatomite from aqueous solutions: Mechanism, isotherm and kinetic studies. *Global NEST Journal,* 18.

SAMSURI, A. W., SADEGH-ZADEH, F. & SEH-BARDAN, B. J. 2014. Characterization of biochars produced from oil palm and rice husks and their adsorption capacities for heavy metals. *International Journal of Environmental Science and Technology,* 11**,** 967-976.

SE, A., GIMBA, C., UZAIRU, A. & DALLATU, Y. 2013. Preparation and characterization of activated carbon from palm kernel shell by chemical activation. *Res. J. Chem. Sci,* 2231**,** 606X.

SELLAOUI, L., DOTTO, G. L., LAMINE, A. B. & ERTO, A. 2017. Interpretation of single and competitive adsorption of cadmium and zinc on activated carbon using monolayer and exclusive extended monolayer models. *Environmental Science and Pollution Research,* 24**,** 19902-19908.

SH. GOHR, M., ABD-ELHAMID, A. I., EL-SHANSHORY, A. A. & SOLIMAN, H. M. A. 2022. Adsorption of cationic dyes onto chemically modified activated carbon: Kinetics and thermodynamic study. *Journal of Molecular Liquids,* 346**,** 118227.

SLATNI, I., ELBERRICHI, F. Z., DUPLAY, J., FARDJAOUI, N. E. H., GUENDOUZI, A., GUENDOUZI, O., GASMI, B., AKBAL, F. & REKKAB, I. 2020. Mesoporous silica synthesized from natural local kaolin as an effective adsorbent for removing of Acid Red 337 and its application in the treatment of real industrial textile effluent. *Environmental Science and Pollution Research,* 27**,** 38422-38433.

SOLTANI, N., SAION, E., HUSSEIN, M. Z., ERFANI, M., ABEDINI, A., BAHMANROKH, G., NAVASERY, M. & VAZIRI, P. 2012. Visible Light-Induced Degradation of Methylene Blue in the Presence of

Photocatalytic ZnS and CdS Nanoparticles. *International Journal of Molecular Sciences* [Online], 13.

SON, G. & LEE, H. 2016. Methylene blue removal by submerged plasma irradiation system in the presence of persulfate. *Environmental Science and Pollution Research,* 23**,** 15651-15656.

SUGUMARAN, P., SUSAN, V. P., RAVICHANDRAN, P. & SESHADRI, S. 2012. Production and characterization of activated carbon from banana empty fruit bunch and Delonix regia fruit pod. *Journal of Sustainable Energy & Environment,* 3**,** 125-132.

SURESH JEYAKUMAR, R. & CHANDRASEKARAN, V. 2014. Adsorption of lead (II) ions by activated carbons prepared from marine green algae: Equilibrium and kinetics studies. *International Journal of Industrial Chemistry,* 5**,** 1-10.

TAŞAR, Ş., KAYA, F. & ÖZER, A. 2014. Biosorption of lead(II) ions from aqueous solution by peanut shells: Equilibrium, thermodynamic and kinetic studies. *Journal of Environmental Chemical Engineering,* 2**,** 1018-1026.

TCHOBANOGLOUS, G. 1991. Wastewater engineering : treatment, disposal, and reuse. *In:* BURTON, F. L. (ed.) 3rd ed. / ed. New York :: McGraw-Hill.

TOLES, C. A., MARSHALL, W. E., WARTELLE, L. H. & MCALOON, A. 2000. Steam-or carbon dioxide-activated carbons from almond shells: physical, chemical and adsorptive properties and estimated cost of production. *Bioresource technology,* 75**,** 197-203.

VASIRAJA, N., PRABHAHAR, R. S. S. & JOSHUA, A. 2023. Preparation and Physio–Chemical characterisation of activated carbon derived from prosopis juliflora stem for the removal of methylene blue dye and heavy metal containing textile industry effluent. *Journal of Cleaner Production,* 397**,** 136579.

WAJI, Y. A. 2018. *Bamboo based activated carbon for removal of lead from aqueous solution.* M. Sc. thesis, Addis Ababa Science and Technology University.

WANG, B., YU, J., LIAO, H., ZHU, W., DING, P. & ZHOU, J. 2020. Adsorption of Lead (II) from Aqueous Solution with High Efficiency by Hydrothermal Biochar Derived from Honey. *International Journal of Environmental Research and Public Health* [Online], 17.

WEBER WALTER, J. & MORRIS, J. C. 1963. Kinetics of Adsorption on Carbon from Solution. *Journal of the Sanitary Engineering Division,* 89**,** 31-59.

XIAO, K., LIANG, S., WANG, X., CHEN, C. & HUANG, X. 2019. Current state and challenges of full-scale membrane bioreactor applications: A critical review. *Bioresource Technology,* 271**,** 473-481.

XU, P. 2018. Research and application of near-infrared spectroscopy in rapid detection of water pollution. *Desalination and Water Treatment,* 122**,** 1-4.

YADAV, S., YADAV, A., BAGOTIA, N., SHARMA, A. K. & KUMAR, S. 2021. Adsorptive potential of modified plant-based adsorbents for sequestration of dyes and heavy metals from wastewater - A review. *Journal of Water Process Engineering,* 42**,** 102148.

YAHYA, M. A., AL-QODAH, Z. & NGAH, C. W. Z. 2015. Agricultural bio-waste materials as potential sustainable precursors used for activated carbon production: A review. *Renewable and Sustainable Energy Reviews,* 46**,** 218-235.

YANG, B., ZUO, J., TANG, X., LIU, F., YU, X., TANG, X., JIANG, H. & GAN, L. 2014. Effective ultrasound electrochemical degradation of methylene blue wastewater using a nanocoated electrode. *Ultrasonics Sonochemistry,* 21**,** 1310-1317.

YANG, L., QIAN, S., WANG, X., CUI, X., CHEN, B. & XING, H. 2020. Energy-efficient separation alternatives: metal–organic frameworks and membranes for hydrocarbon separation. *Chemical Society Reviews,* 49**,** 5359-5406.

YAO, S., ZHANG, J., SHEN, D., XIAO, R., GU, S., ZHAO, M. & LIANG, J. 2016. Removal of Pb(II) from water by the activated carbon modified by nitric acid under microwave heating. *Journal of Colloid and Interface Science,* 463**,** 118-127.

YOGALAKSHMI, K. N., DAS, A., RANI, G., JASWAL, V. & RANDHAWA, J. S. 2020. Nano-bioremediation: a new age technology for the treatment of dyes in textile effluents. *Bioremediation of Industrial Waste for Environmental Safety.* Springer.

YOUSSEF, A. M., EL-NAGGAR, M. E., MALHAT, F. M. & EL SHARKAWI, H. M. 2019. Efficient removal of pesticides and heavy metals from wastewater and the antimicrobial activity of f-MWCNTs/PVA nanocomposite film. *Journal of Cleaner Production,* 206**,** 315-325.

YUE, Y., ZHANG, P., WANG, W., CAI, Y., TAN, F., WANG, X., QIAO, X. & WONG, P. K. 2020. Enhanced dark adsorption and visible-light-driven photocatalytic properties of narrower-band-gap Cu2S decorated Cu2O nanocomposites for efficient removal of organic pollutants. *Journal of hazardous materials,* 384**,** 121302.

ZAHRIM, A. Y., TIZAOUI, C. & HILAL, N. 2011. Coagulation with polymers for nanofiltration pre-treatment of highly concentrated dyes: a review. *Desalination,* 266**,** 1-16.

ZAKI, A. A. & EL-GENDY, N. A. 2014. Removal of metal ions from wastewater using EB irradiation in combination with HA/TiO2/UV treatment. *Journal of Hazardous Materials,* 271**,** 275-282.

ZENG, Y., TANG, X., QIN, Y., MAIMAITI, A., ZHOU, X., GUO, Y., LIU, X., ZHANG, W., GAO, J. & ZHANG, L. 2023. Enhanced removal of methylene blue from wastewater by alginate/carboxymethyl cellulose-melamine sponge composite. *International Journal of Biological Macromolecules,* 244**,** 125280.

ZHANG, J., PING, Q., NIU, M., SHI, H. & LI, N. 2013. Kinetics and equilibrium studies from the methylene blue adsorption on diatomite treated with sodium hydroxide. *Applied Clay Science,* 83**,** 12-16.

ZHOU, N., CHEN, H., XI, J., YAO, D., ZHOU, Z., TIAN, Y. & LU, X. 2017. Biochars with excellent Pb(II) adsorption property produced from fresh and dehydrated banana peels via hydrothermal carbonization. *Bioresource Technology,* 232**,** 204-210.